A comparative study of oregano (*Origanum vulgare* ~~L.)~~ L.) essential oil-based polycaprolactone nanocapsules/microspheres: Preparation, physicochemical characterization, and storage stability

> (i) The corrections made in this section will be reviewed and approved by journal production editor.

Asma Fraj[a],* asma.fraj@enim.rnu.tn, Fadhel Jaâfar[a] jaafarfadhel@gmail.com, Meritxell Marti[b] meritxell.marti@iqac.csic.es, Luisa Coderch[b] luisa.coderch@iqac.csic.es, Neji Ladhari[a] neji.ladhari@isetkh.rnu.tn

[a]Textile Engineering Laboratory of ISET Ksar Hillel, BP 68, Street Hadj Ali Soua, Ksar Hellal 5070, University of Monastir, Tunisia

[b]~~Textiles and Cosmetic Innovations, Institute of Advanced Chemistry of Catalunya (IQAC-CSIC), c/ Jordi Girona 18-26, 08034, Barcelona, Spain~~Textiles and Cosmetic Innovations, Institute of Advanced Chemistry of Catalonia (IQAC-CSIC), c/ Jordi Girona 18-26, 08034, Barcelona, Spain

*~~Cprresponding author.~~

*Corresponding author.

Abstract

Essential oils have been used in clinical therapies and healing practices for several chronic diseases, but it is still challenging their extent use due to their poor stability. Nanotechnology delivery systems have been proposed as an alternative to improve their stability. Oregano (*Origanum vulgare* ~~L.~~ L.) is one of the most important medicinal plant highly reputed as an efficient remedy for infectious diseases. This study proposes the use of polycaprolactone, a biodegradable polymer, as a wall material for the encapsulation of *Origanum vulgare* ~~L.~~ L. essential oil, a carvacrol-rich source, using the nanoprecipitation and double emulsion methods. Nanocapsules formulations showed different values of mean particle size ranged between 175.17 ± 0.31 nm and 220.93 ± 2.73 nm, negative zeta potential values ranged between ~~-18.7 0.50 mV up to~~ -18.7 ± 0.50 mV up to -42.53 ± 1.01 mV, and encapsulation efficiencies ranging from

50.36±1.86% and 85.89±2.40%. The optimized nano-formulation presented a nano-scale size of 181.6±2.17 nm, a monomodal size distribution with a polydispersity index of 0.133±0.01, a pH value of 4.92 and a zeta potential value of ~−40.9±0.93 mV. The encapsulation efficiency of 85.89±2.40% was achieved. In addition, microspheres produced by double emulsion, demonstrated porous microspheres morphology in the size of 1759.00±162.6 nm, pH value of 5.98, a zeta potential value of ~−15.7±1.56 mV and encapsulation efficiency of 47.52±0.52%. Dynamic light scattering and scanning electron microscopy were performed to verify the size and the colloidal morphology. Thermal properties were assessed by thermogravimetric analysis and differential scanning calorimetry and the measurements revealed the thermal stability of the particles and showed that the crystalline state was less ordered in nanocapsules. Attenuated Total Reflectance Fourier Transform Infrared results indicated a slight shift in the C=~~=O band of the polymer from 1723 cm~~ O band of the polymer from 1723 cm=[1] induced by the change in its crystallinity degree due to the successful incorporation of oregano within its shell. Moreover, the long-term stability study was carried out for a period of 60 days at 4±2 °C, 25±2 °C and 40±2 °C. Results showed that nanocapsules were physically stable with high carvacrol retention at different temperatures. However when microspheres were thermally treated at 25 °C and 40 °C, an increase in particle size was observed. Besides, carvacrol retention decreased to 64.56% and 61.84% at 25 °C and 40 °C, respectively. From gathered results, the good physical stability of nanocapsules in long-term storage with high carvacrol retention stability were observed mainly at 4 °C.

1 Introduction

From historical times, plants' roots, stem, and leaves have been used as remedies and treatments for skin diseases (Atul Bhattaram et al., 2002). Nowadays, herbal medicinal products utilization is steadily increasing due to their healing therapeutic potentials, their safe toxicological profiles, and their improved microbial safety (Ekor, 2014; Sharifi-Rad et al., 2017; Wegener, 2017). ~~Wegener, 2017)~~.

Essential oils, derived from aromatic plants, are complex mixtures of compounds mainly composed of terpenoids and phenolic acids. There is a substantial literature concerns the use of essential oils in pharmaceutical and cosmetic industries (Sarkic et al., 2018), as food preservatives (Oliveira et al., 2017), as insecticides in agriculture (Nasr et al., 2017), and in the medical textile industries (Dhivya et al., 2015; Massaroni et al., 2015; Mečņika et al., 2014). Essential oils and their volatile constituents have been previously proved to exert a broad- spectrum of therapeutic potentials (Islam et al., 2016; Shaaban et al., 2012) ~~Shaaban et al., 2012)~~, as such, their medicinal use is related to their biologically active substances with potent pharmacological activities (Jütte et al., 2017; Teixeira et al., 2013a).

Origanum vulgare ~~L.~~ L., commonly known as oregano, is an endemic shrub of the Lamiaceae family native to the Mediterranean region (Almeida et al., 2013; Elshafie and Camele, 2016). The *Origanum vulgare* ~~L.~~ L.

essential oil (OEO) spread in all Balkans is composed of different amounts of compounds such as monoterpene hydrocarbons (α-pinene, β-pinene, p-cymene), sesquiterpenes (β- caryophyllene), Linalool, terpinen-4-ol, and phenols (carvacrol, thymol). The main oregano component, carvacrol, makes up to 68% of the total oil composition. Carvacrol is generally recognized as safe (GRAS) by the U.S. Food and Drug Administration (FDA) as a food additive which attests its safety and non-toxic nature (Regulation number of the United States Code of Federal Regulations 172.515) (Suntres et al., 2015; Zotti et al., 2013).

Origanum vulgare ~~L.~~ L. has shown potent antimicrobial activities against several plants and human pathogens. Numerous studies have reported the significant inhibitory activity of OEO and its components against some phytopathogenic fungi such as *Phytophthora citrophthora* (R.E. Sm. & E.H. Sm.) Leonian, *Botrytis cinerea* Pers., *Penicillium italicum* Wehrner, *Penicillium expansum* Link, *Rhizopus stolonifer* (Ehrenb.) Vuill., (Camele et al., 2012), *Pectobacterium* spp. and *Pseudomonas* spp. (Božik et al., 2017). *Origanum vulgare* ~~L.~~ L. phenolic constituents carvacrol and thymol have shown a promising inhibition of the brown rot of peach fruits caused by *Monilinia laxa*, *Monilinia fructigena*, and *Monilinia fructicola in vitro* and *in vivo* (Elshafie et al., 2015; Elshafie and Camele, 2016). Furthermore, the antibacterial activity of OEO against a number of plant pathogens has been reported by (Adebayo et al., 2013). These pathogens include *Aspergillus niger* van Tieghem, *Aspergillus flavus* Link, *Aspergillus ochraceus* Wilhelm, *Fusarium oxysporum* Snyder and Hansen, *Penicillium* sp. L., *Pseudomonas aeruginosa* Schroter ATCC 2730, *Staphylococcus aureus* Rosenbach ATCC 6538, *Fusarium solani* var. *coeruleum* (Martius) Saccardo, *Clavibacter michiganensis* S., *Phytophthora infestans* Mont., *Sclerotinia sclerotiorum* Lib. and *Xanthomonas vesicatoria* D. Moreover, the effectiveness of OEO in inhibiting *Escherichia coli*, *Staphylococcus aureus*, *Bacillus megaterium* de Bary ITM100, *Enterococcus faecalis*, *Klebsiella pneumoniae* and *Pseudomonas aeruginosa* was tested (Elshafie et al., 2017; Man et al., 2019; Martucci et al., 2015; Swamy et al., 2016; Vattem et al., 2005). Many authors have, recently, focused on OEO potential healing of skin diseases (Orchard and van Vuuren, 2017), and have shown antimalarial (El Babili et al., 2011), antioxidative activity (Olmedo et al., 2014; Teixeira et al., 2013b) and anticancer activity (Han and Parker, 2017), mainly due to its high content on carvacrol which stands out as the active antimicrobial and antioxidant phenol (Saeed and Tariq, 2009; Silva et al., 2012; Wang et al., 2017).

Encapsulation of plant bioactive compounds such as essential oils and monoterpenes within biodegradable delivery systems could have the potential to overcome the susceptibility of essential oils, increase their aqueous solubility, promote their stability during thermal processing and storage, thereby enhancing their applicability and improves their pharmacological activity (de Matos et al., 2019). A variety of delivery systems carriers for bioactive compounds include polymeric micelles, liposomes, nanoemulsion, lipid particles, polysaccharides, and polymeric nano-microparticles have been developed (Pimentel-Moral et al., 2016). These systems offer the opportunity to deliver bioactive molecules at a controlled rate and for a targeted site. Recent advances in research on essential oils administration through the skin were achieved (Ruela et al., 2016). ~~(Ruela et al., 2016).~~ Since the major challenge in clinical practice is addressing and controlling the bioactive agent release to the targeted site, the quantitative evaluation of the percutaneous absorption of essential oils was performed in order to predict their mechanism of action and their activity in the skin (Bilia et al., 2014; Casanova and Santos, 2016). In this regard, the incorporation of OEO, a health-promoting substance, in solid matrices has garnered much attention thanks to their biological activities and their anti-inflammatory efficacy. *Origanum vulgare* ~~L.~~ L. essential oil was encapsulated into chitosan (Hosseini et al., 2013), inulin (Beirão-da-

Costa et al., 2013; Beirão da Costa et al., 2012), starch (Almeida et al., 2013), and recently, nonwoven loaded with alginate microcapsules for agriculture use has been evaluated (Ferrándiz et al., 2017). Likewise, the encapsulation of carvacrol, the main component of oregano, has been extensively studied (Guimarães et al., 2015; Hussein et al., 2017; Liu et al., 2016).

Among many biodegradable polymers, the aliphatic polyester polycaprolactone (PCL) can be considered as a better candidate for the design of micro and nanoconstructs to deliver various natural therapeutic agents. PCL has been widely adopted as a suitable biomaterial due to its high thermal stability, its relatively slow degradability and good biocompatibility, which eases its use as a model polymer. In addition to that, PCL is a hydrophobic polymer with excellent elastic properties; it possesses a wide range of interesting features including chemical resistance, low water absorption which makes it a promising component in biomedical applications (Cerkez et al., 2017; Mirbagheri et al., 2017), particularly in the medical bio-textiles (Gupta and Moghe, 2013; Jung et al., 2016; Malikmammadov et al., 2018). PCL micro and nanoparticulate systems have gained attention and proved to be potential alternatives for many therapeutic approaches (Baek et al., 2016; Pohlmann et al., 2013). This interest is due to numerous benefits offered by these systems which have been successfully used for encapsulation of many actives for subcutaneous delivery thanks to their ease of application, their established biocompatibility and biodegradability and localized delivery for site-specific action (Çırpanlı et al., 2011; Feng et al., 2012). The development of effective particulate delivery systems is important in clinical and experimental medicine. In fact, generating stable and size-controlled polymeric particles with a narrow size distribution plays an important role in promoting biological activity, enhancing the targeting efficacy and therapeutic efficiency (Hickey et al., 2015). Generally, the particle size monitoring has been shown to have a significant influence on bioactive delivery into the skin *in vivo* (Gupta and Rai, 2017; Stander et al., 2018; Verma et al., 2003). Therefore, controlling the preparation method, physicochemical properties and storage stability is crucial when preparing particles with desired size and properties. A wide array of therapeutics used for transdermal delivery systems such as patches, ointments, and creams have shown promise in enhancing the skin permeation of lipophilic active agents with low molecular weight and low doses. Generally, microspheres with a diameter of 2000 nm or above were not able to deliver the encapsulated material into deeper layers of the skin and have shown maximum deposition of the active principle contents in the stratum corneum (Martí et al., 2014). However, nanocapsules with a diameter of 200 nm have shown the ability to deliver their contents into the deeper skin layers (Badri et al., 2018).

Accordingly, the development of a long-acting formulation of oregano is foreseen thanks to the potential hydrophobic property of PCL polymer which confers the ability to release the bioactive natural compound for extended periods of time. The nanoprecipitation is commonly used to encapsulate both hydrophilic and hydrophobic bioactive molecules, yielded higher encapsulation efficiency with the long-term stability of the core and higher sustained-release (Martínez Rivas et al., 2017; Miladi et al., 2016). The nanoprecipitation is a simple and effective technique which doesn't require high stirring rates and temperatures conditions. Moreover, it allows obtaining small nanoparticles around 100–200 nm with narrow and a monomodal distribution. The double emulsion method was first described by Seifriz (1924) and was described as a complex system in which droplets are dispersed in a continuous phase and contain smaller dispersed droplets themselves. Double emulsion systems were used to encapsulate both hydrophobic and hydrophilic compounds

and they were considered as promising delivery systems in industrial areas of cosmetics and medical textiles (Carreras et al., 2013; Martí et al., 2014).

In view of this background, we propose a comparative study for the preparation of polycaprolactone-loaded *Origanum vulgare* ~~L.~~ L. essential oil. For this, we investigated two different preparation methods (the nanoprecipitation and the double emulsion) and a number of variables that could potentially influence the encapsulation of hydrophobic essential oil in terms of size range and distribution, encapsulation efficiency and stability during storage. Physicochemical characteristics and the thermal behavior of both systems were, further, studied. The stability of storage was ascertained in various simulated temperatures and time to evaluate their effects on the physicochemical and total carvacrol retention (CAR%) under these different storage conditions. This study was considered valuable for producing stable polymeric systems loaded-oregano essential oil with significant carvacrol retention capability. These improved stability systems will serve in pharmaceutical and cosmetical industries and will be highly beneficial for the treatment of topical cutaneous diseases.

2 Materials and methods

2.1 Materials

Polycaprolactone (PCL) (average molecular weight of 45 000), poly (vinyl alcohol) (PVA), (87–89% hydrolyzed, MW 31 000–50 000 Da) were procured from Sigma–Aldrich Chemicals Private Ltd. (Madrid, Spain). Oregano Essential Oil (OEO), obtained from (Terpenic lab, Barcelona Spain), was used as the core material. Polysorbate 80 (Tween® 80) and Sorbitan monooleate (Span® 80), obtained from Sigma–Aldrich Chemicals Private Ltd. (Madrid, Spain), were employed as stabilizing agents in nanocapsules preparation. Acetone and dichloromethane (DCM), purchased from Sigma-Aldrich, were used as organic solvents for PCL. Solvents including acetonitrile and methanol in HPLC grade (Fisher Scientific,) were used for HPLC analysis. Nylon filters, pore size 0.45 µm (Millipore, USA) were used for the filtration of solvents and prepared samples for HPLC analysis. All other solvents used in this work were of analytical grade and acquired from Sigma-Aldrich, Spain. Milli-Q water was used throughout the work.

2.2 Methods

2.2.1 Preparation of nanocapsules by nanoprecipitation

Oregano nanocapsules (PCL-OEO-NCs) were prepared ~~via~~ via nanoprecipitation of the pre-formed polymer (interfacial deposition/solvent displacement) reported by Fessi et al. (1989). In the first step, PCL forming the organic phase (100 mg) was dissolved in acetone solution (27 mL) by mild heating (60 °C) for 15 min. Oregano essential oil (OEO) and a low-HLB surfactant (Span® 80, HLB = 4.3) (a hydrophilic-lipophilic balance that allows stable and size-controlled nanocapsules) were mixed to the resulting solution. Further, the polymer-OEO mixture solution was gently added dropwise into 55 mL aqueous solution of a high-HLB surfactant (tween® 80, HLB = 15), under moderate magnetic stirring for 10 min. Acetone and part of water were removed in a rotary evaporator at 40 °C, adjusting for a final volume of 55 mL. Empty nanocapsules (PCL-NCs) were prepared ~~via~~ via the same process. The different formulations are presented in Table 1.

The composition of formulations prepared by nanoprecipitation.

| Formulations | Components | | | | | | |
| | Organic phase | | Aqueous phase | | | Operating conditions | |
	PCL/OEOratio	Acetone(mL)	Span 80(mg)	Tween 80(mg)	Milli-Q water (mL)	Stirrer speed(rpm)	Organic phase injection speed (min)
PCL-NCs	1/0	27	76.6	76.6	55	500	30
PCL-OEO-NCs$_1$	1/3.2	27	76.6	76.6	55	500	30
PCL-OEO-NCs$_2$	1/3.4	27	76.6	76.6	55	500	30
PCL-OEO-NCs$_3$	1/4	27	76.6	76.6	55	500	30

2.2.2 Preparation of microspheres by double emulsion

Oregano microspheres (PCL-OEO-MSs) were prepared by $O_1/O_2/W$ double emulsion method (Carreras et al., 2013). This process involves the preparation of (O_1/O_2) at a first stage, followed by addition of an excess volume of water to facilitate the diffusion of the organic solvent into the external aqueous phase. Briefly, 0.3% (w/v) of oregano essential oil in mono-alcohol was added dropwise into a solution of 0.3% (w/v) PCL in dichloromethane. The simple emulsion was mixed vigorously by mechanical agitation (ULTRA-TURRAX T25, IKA) for 30 min at 24 000 rpm to form an O_1/O_2 phase. This resultant primary emulsion (O_1/O_2) was, then, injected drop by drop into a beaker containing the 2% (w/v) aqueous PVA solution while emulsified at 24,000 rpm for 20 min at 4 °C until the formation of a double emulsion. The $O_1/O_2/W$ emulsion was performed to evaporate the organic solvent at the water/air interface by stirring for 24 hours at 400 rpm to obtain microspheres. Empty microspheres (PCL-MSs) were prepared ~~via~~ *via* the same process. The volume of the solution was weighed before and after evaporation to ensure the evaporation of the organic solvent. Both prepared formulations are presented in Table 2.

The composition of formulations prepared by double emulsion.

Formulations	Components						
	Organic phase		Aqueous phase			Operating conditions	
	PCL/OEOratio	DCMvolume (mL)	Monoalcohol (mL)	PVA(%)	Milli-Q water(mL)	Stirrer speed(rpm)	Organic phaseinjection speed (min)
PCL-MSs	1/0	15	25	2	100	24000	30
PCL-OEO-MSs	1/1	15	25	2	100	24000	30

2.3 Characterization of the prepared particles

2.3.1 Particle size, polydispersity index, and Zeta potential measurements

The hydrodynamic size (PS), the polydispersity index (PDI), and the zeta potential (ZP) were performed immediately by dynamic light scattering (DLS) using a Nano ZS Zetasizer ZEN3600 (Malvern Instruments Ltd., Malvern, Worcestershire, UK). The zeta potential was measured by electrophoretic mobility considering the water dielectric constant of 78.5. The polydispersity index was measured in order to describe the broadness of the particle size distribution calculated from the cumulants analysis. All samples were dispersed in Milli-Q water (1:100, v/v), and were measured at room temperature of 25 °C. Each sample was performed in triplicate. The data were obtained in mean value and expressed as a $\pm$ standard deviation.

2.3.2 Determination of carvacrol content

The carvacrol retention profile and quantification analyses were processed using the HPLC chromatograph (Shimadzu, Japan) equipped with a C18 (Microsorb) analytical column (5 μm, 250×4.6 mm) and coupled to an SPD-M20A diode array detector.

Carvacrol content was determined after extraction from the formulations using acetonitrile (5 mL). All samples were maintained in ultrasound for 60 min, centrifuged for another 15 min and then the supernatant was filtrated and analyzed by HPLC. The samples were filtered before the injection in the HPLC with nylon filters, pore size 0.45 μm (Millipore, USA). The absorption spectrum revealed a maximum peak of oregano essential oil absorbance at 274 nm. The UV detector was set where the chromatograms were processed at an absorption wavelength of 274 nm. Data acquisition and processing were performed and all samples were isocratically run with a mobile phase composed of acetonitrile-water (60:40, v/v). The injection volume was 20 μL, and the retention of carvacrol was approximately 7 min at a flow rate of 1.0 mL/min. The column oven temperature was maintained at 25 °C. For the carvacrol quantification, a standard curve was developed with a

determination coefficient ($r^2 = 0.9998$) using standard solutions of carvacrol (134.5 µg/mL to 0.108 µg/mL). All measurements were performed in triplicate.

2.3.3 Encapsulation Eefficiency (EE%)

The encapsulation efficiency (EE%) of PCL-OEO-NCs and PCL-OEO-MSs, was determined using the spectrophotometric method. The nanocapsules pellet (PCL-OEO-NCs) was separated from none encapsulated free essential oil by centrifugation at 9000 rpm at 4 °C for 15 min. The supernatant was removed and separated nanocapsules were redispersed and washed for a triple in Milli-Q water by centrifuging at 9000 rpm at 4 °C for another 5 min. The pellet of each nanocapsules formulation was extracted using methanol as an extracting solvent, vortexed vigorously and centrifuged. The extracted oil was collected and quantified spectrophotometrically at 274 nm.

Encapsulation Efficiency (EE%) of PCL-OEO-MSs, was determined by centrifugation of microspheres formulations with 18,100 rpm at 4 °C for 15 min. The pellet was separated from the aqueous medium containing the non-associated oil and then collected, washed for a triple in Milli-Q water and centrifuged at 18,100 rpm at 4 °C for another 5 min. Methanol was added to the washed pellet, vortexed and further centrifuged for 10 min.

The extracted oil was quantified using a high-performance liquid chromatography diode array detection (HPLC–DAD) and ultraviolet (UV)–spectrophotometry (CARY 300). HPLC–DAD analyses were conducted using a C18 (Microsorb) analytical column, isocratic elution with acetonitrile-water (80:20 (v/v)) mobile phase at 1.0 mL/min flow rate and detection at 274 nm. The calibration curve was obtained using linear regression where y is the absorption, and x is the concentration of essential oil in the solution. The linear response ($r^2 = 0.9998$) was obtained within a concentration range of 134.5 µg/mL to 0.108 µg/mL using HPLC–DAD, and in the working range of 100 µg/mL to 0.781 µg/mL with linear correlation coefficient ($r^2 = 0.9985$) using spectrophotometry. All the points from the calibration curve were obtained in triplicate. Both methods were suitable to be applied for the determination of loading capacity percentage and encapsulation efficiency.

Calibration curves with concentration ~~versus~~ versus absorbance were plotted for each method and the obtained data were subjected to regression analysis using the least-squares method.

The encapsulation efficiency (EE%) and the actual loading capacity (LC%) were calculated according to Equations Eq~~. (1) and Eq.~~s. (1) and (2).

The encapsulation efficiency (EE%) was calculated from the division of the OEO content recovered by methanol extraction by the theoretical oil content. Encapsulation efficiency (EE%) was calculated by using the direct following equation [Eq. (1)] :

$$EE\% = \frac{Actual\ OEO\ loaded}{Theoretical\ OEO\ loading} \times 100$$

(1)

$$LC\% = \frac{OEO\ mass\ in\ particles}{Mass\ of\ particles} \times 100$$

(2)

2.3.4 Scanning electron microscopy (SEM)

The scanning electron microscope (SEM) type Hitachi instruments TM-1000 was used to study the morphology of the nano-microparticles. The suspensions were separated from the liquid by centrifugation and dispersed in Milli-Q water. One drop of each dispersion was placed on a carbon adhesive disc, dried at room temperature for 24 h and then fixed on an aluminum mounting pin. Samples were imaged by Hitachi instruments type TM-1000 which use low-vacuum observation techniques combined with high sensitivity backscattered electron detector and allow even non-conductive samples to be observed as is, with no need to apply metallic coatings. The dried nano-microparticles were, then, examined and a representative SEM image was reported.

2.3.5 Thermal analyses

The thermal properties of the PCL-OEO-NCs$_1$ and PCL-OEO-MSs and their individual compounds were analyzed by TGA and DSC. Thermogravimetric analysis (TGA) was performed with a TGA instrument (Model TGA/SDTA 851^e; Mettler Toledo), with STARe software (version SW 9.30). Approximately 5.00 ± 0.1 mg of each sample was weighted (depending on the sample) by using a microbalance (XPR2, Mettler Toledo). They were packed into an aluminum pierced pan (100 µL) and were, then, heated under a nitrogen stream (50 mL/min) from 25 °C to 550 °C at a heating rate of 10 °C/min.

Differential scanning calorimetry (DSC) experiments were performed using a heat flux DSC instrument (DSC-821, Mettler Toledo) under nitrogen stream (50 mL/min.). Approximately 3 mg ± 0.5 of the sample were weighted (depending on the sample) using a microbalance (XPR2, Mettler Toledo). They were packed into an aluminum pierced pan (40 µL), the pan was hermetically sealed and heated from 0 °C to 150 °C at a rate of 10 °C/min under a nitrogen atmosphere at a flow rate of 20 mL/min. An empty pan was used as a reference.

2.3.6 ATR-FTIR assessment of the particles

The Attenuated Total Reflectance Fourier Transform Infrared (ATR-FTIR) spectroscopy was performed to investigate the functional groups present in PCL-OEO-NCs$_1$ and PCL-OEO-MSs. The solid-state samples were placed for spectra recording on a NICOLET AVATAR 360 FTIR Spectrophotometer (Nicolet Instruments, Inc., Madison, WI, USA) equipped with an attenuated total reflection (ATR) sampling accessory that used a diamond with an angle of incidence of 45° in a horizontal orientation. Spectra were obtained in the 500-~~4000 cm-~~ $4000\ cm^{-1}$ wavenumber range with an average of 32 scans using a resolution of 4 cm^{-1}. The advanced ATR correction algorithm introduced in OMNIC software Version 7.3 (Nicolet, Madison, WI, USA) was used to analyze the spectra, read the peak position and correct band intensity distortion, peaks shifts and polarization effects. Analysis of every sample was made in triplicate. All measurements were carried out at room temperature under ambient conditions.

2.3.7 Accelerated stability ~~T~~test

In order to assess the storage conditions impact on PCL-OEO-NCs$_1$ and PCL-OEO-MSs formulations, the obtained suspensions were stored and protected from daylights irradiation in hermetically sealed amber bottles. The samples were subjected to three different storage temperatures: $4 \pm 2\,°C$ (refrigerator), $25 \pm 2\,°C$ (room temperature) and $40 \pm 2\,°C$ (oven) with 60% RH in a stability testing chamber, and monitored after 24 h, 7, 15, 30 and 60 days, in triplicate. For the predetermined period and in the mentioned conditions, the samples were carried out, in triplicate, for their visual, physio-chemical characteristics such average diameter, polydispersity index, zeta potential, pH, and carvacrol retention (CAR%).

2.3.8 pH determination

The determination of the hydrogen potential (pH) was performed directly on the suspensions, in a pH meter-Radiometer Copenhagen potentiometer previously calibrated with pH 4.0 and 7.0 buffer solutions. The pH was evaluated during the stability test.

2.3.9 Statistical analysis

Statistical analysis of data was performed by one-way analysis of variance (ANOVA), using GraphPad Prism 6.01 software compared by Tukey's test and assuming confidence level of 95% for statistical significance. All the results were expressed as mean $\pm$ standard deviation S.D. Principal Component Analysis (PCA) was used to study the relationship between all of the variables cited in the manuscript. All statistical analyses were performed with XLSTAT software (v.2019.1, Addinsoft, USA). Pearson correlation coefficients were calculated when needed between correlated variables.

3 Results and discussion

3.1 Optimization and characterization of PCL-OEO-NCs

PCL nanocapsules were successfully prepared using the nanoprecipitation method of the interfacial deposition of the preformed polymer method patented by Fessi et al. (1989). The choice of the nanoencapsulation process depends on the polymer to be applied and necessarily the solubility of the active compound to be encapsulated which is considered as an important factor affecting the loading capacity of the carrier system (Kalepu and Nekkanti, 2015).

The nanoprecipitation is a very used method for the preparation of polymeric nanocarriers with therapeutic index. This process is widely adopted to encapsulate hydrophobic cores, such as essential oils, into polymeric matrices. The nanoprecipitation processing simplicity and reproducibility allows the ease of scale-*up* and obtaining nanoparticles with narrow size distribution. The preparation method allows obtaining reproducible metastable NCs dispersions yielded higher encapsulation efficiency with the higher stability of the core and an important sustained-release (Martínez Rivas et al., 2017; Miladi et al., 2016).

In this study, OEO-loaded PCL nanocapsules were produced using the nanoprecipitation method and their physicochemical characterization was analyzed by DLS where the particle size (PS), the zeta potential (ZP), polydispersity index (PDI), and encapsulation efficiencies (EE%) were determined (Fig. 1, Table 3).
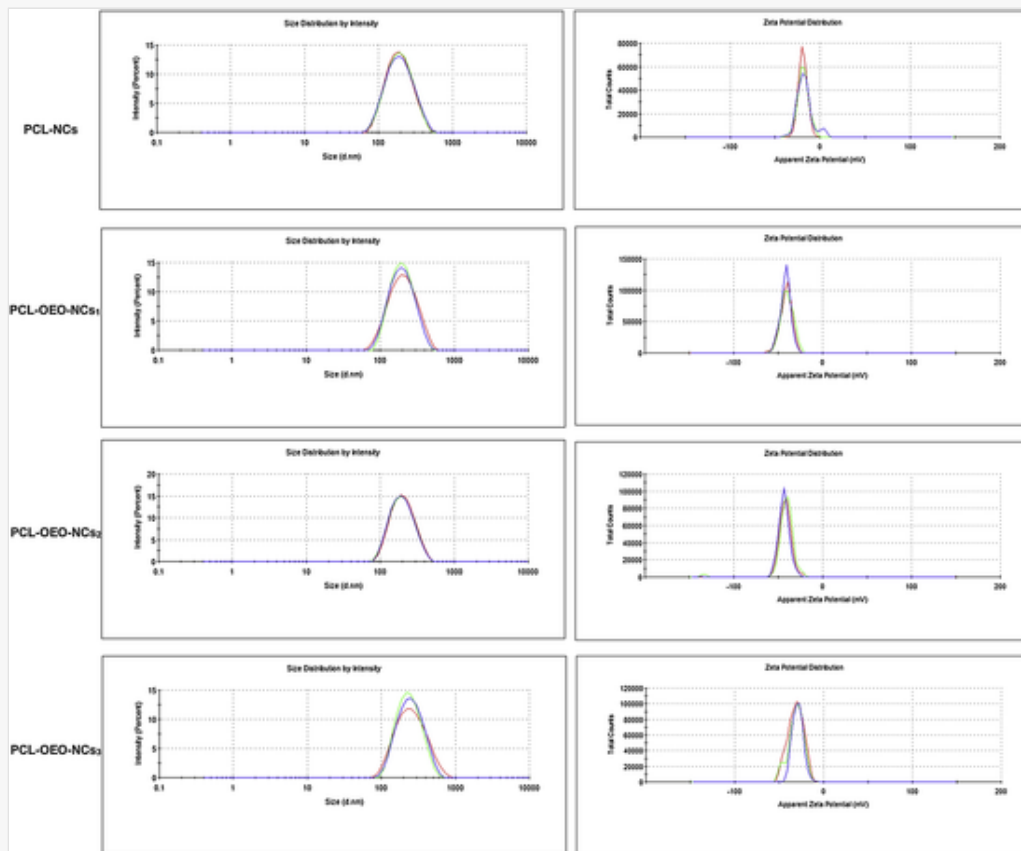
Particle size and zeta potential distribution of nanocapsules formulations.

alt-text: Table 3

Table 3

ⓘ The presentation of Tables and the formatting of text in the online proof do not match the final output, though the data is the same. To preview the actual presentation, view the Proof.

Initial experimental results of the nanocapsules expressed as mean $\pm$ SD.

Formulations	PCL/ OEO ratio	PS^a (nm)	PDI^b	ZP^c (mV)	EE^d (%)	Appearance
PCL-NCs	1/0	175.17±0.31	0.140±0.01	~~−18.70 0.50~~ −18.70±0.50	=	Milky suspension
PCL-OEO-NCs$_1$	1/3.2	181.60±2.17	0.133±0.01	−40.90±0.93	85.89±2.40	Milky suspension
PCL-OEO-NCs$_2$	1/3.4	186.93±1.63	0.144±0.01	−42.53±1.01	68.48±1.53	Milky suspensionOils

						droplets on the surface
PCL-OEO-NCs$_3$	1/4	220.93±2.73	0.178±0.02	−30.67±1.27	50.36±1.86	Milky suspensionOils droplets on the surface

Values are the mean ± SD.

Table Footnotes

[a] ~~Particle size~~Particle size.

[b] ~~Polydispersity IndexcZeta Potential~~Polydispersity Index.

Zeta Potential.

[d] Encapsulation Efficiency.

The nanoencapsulation process was optimized using different conditions and the polymer to the oil ratio (PCL/OEO) was changed while the operating conditions were kept constant. Thence, the appropriate concentration of PCL, OEO, and surfactants was determined experimentally.

The colloidal NCs dispersions were obtained with a transparent to opalescent bluish aspect presenting a Tyndall effect. Unloaded-NCs (PCL-NCs) presented a size diameter of 175.17 ± 0.31 nm, a polydispersity index PDI (0.14 ± 0.01) and ZP (-18.7 mV ± 0.5 mV). During the preparation, a small increment of oregano essential oil (OEO) content promoted changes in the mean size values and surface charge values of the nanocapsules. Obviously, the PCL-OEO-NCs presented mean size values of 181.60 ± 2.17 nm and 186.93 ± 1.63 nm for PCL-OEO-NCs$_1$ and PCL-OEO-NCs$_2$, respectively. In this case, the highest OEO content has led to more negatively charged nanocapsules. PCL-OEO-NCs$_1$ presented $85.89 \pm 2.40\%$ encapsulation efficiency, although, a decrease in oregano content has been demonstrated with PCL-OEO-NCs$_2$. Indeed, processing under the same conditions with only a small increase in oregano oil concentration has led to oiling off and the nanocapsules were obtained with a lower encapsulation efficiency. Whereas, the increase of the polymer to OEO ratio while keeping constant surfactant concentrations generated particles with slightly larger diameter 220.93 ± 2.73 nm for PCL-OEO-NCs$_3$ (Table 3).

Besides, the formulations presented a monomodal particle size distribution, as also confirmed by the obtained low PDIs (< 0.2), confirming the presence of a monodispersed system. The size and PDI values were very similar among nanoparticles of the prepared suspensions. Similar results were reported by Ephrem et al. (2014), who have reported the preparation of rosemary essential oil nanocapsules at a small and a large scale with the nanoprecipitation method. The nanoparticles showed mean diameter values of 220 ± 10 nm to 530 ± 20 nm and PDI values of 0.19 ± 0.01 and 0.31 ± 0.04, respectively. In general, lower PDI values indicate high homogeneity in the particle population, the stability and narrow distribution of formulations (Danaei et al., 2018). However, the increase in PDI value (> 0.2) can generate a relatively heterogeneous population of particles. Thus, the obtained results demonstrated that upon increasing the polymer/ OEO weight ratio, the particle size increases when other formulation variables are kept constant, thereby, suggesting that varying the polymer to OEO weight ratio can affect the size and the PDI values. Inversely, the decline of PDI obtained

with the decreasing of polymer/ OEO weight ratio is attributed to the fact that as the polymer concentration increased, the amount of nanoparticles per unit volume will be small which would favor the formation of the desired monodisperse system (small PDI) as a result of disallowing particle agglomeration (Khalifa et al., 2017).

Additionally, the measurement of zeta potential (ZP) is important to reveal the physical stability of the nano-suspensions and can depend on the concentration and molecular weight of the applied polymer and surfactants in the aqueous phase. ZP or the particle charge, also known as the electrokinetic potential, is the potential at the slipping/shear plane of a colloid particle moving under electric field (Bhattacharjee, 2016; Kaszuba et al., 2010). The zeta potential values are usually determined by the electrophoretic light scattering and can be negative or positive. But, a zeta potential of $+/-30\,mV$ is often used as a stability threshold. In general, higher negative zeta potential values ensure greater electrostatic repulsion forces among the nanoparticles and this repulsion leads, thereafter, to greater separation distances between the nanoparticles in the suspension, reducing neighboring nanocapsules or occasional aggregation caused by Van der Waals interactions. The zeta potential also can be used to determine whether a charged active material is encapsulated within the center of the nanoparticle or on the surface (Honary and Zahir, 2013a, 2013b).

In this case, high negative zeta potential values were observed for all nanocapsules suspensions (Table 3), revealing that the reproducibility of the different batches results in high negative zeta potential values, reflecting kinetically stable formulations. The said stability is generated by an electrostatic repulsion effect resulting from surface charge density which contributes to avoiding aggregation of the hydrophobic colloidal particles dispersed in the aqueous phase. Indeed, the polymer PCL presents $-COOH$ ends groups at the polymer extremities, causing an acid-base balance forming carboxylates, which make the surface negatively charged. Likewise, these negative charges of the ionized carboxylic groups $-COO^-$, promote the stability of the nanocapsules by electrostatic repulsion (Magenheim and Benita, 1991). ~~(Magenheim and Benita, 1991).~~ The zeta potential is also a function of stabilizers nature that control the surface charge of the nanocapsules. Here, the high negative values can be associated with the electrostatic stabilization mechanism due to the presence of the polysorbate 80 (Palla and Shah, 2002). In fact, the use of the non-ionic amphiphilic stabilizer such as tween 80 improves the nanoemulsion stability, due to its hydrophilic polyoxyethylene head groups. This stabilizer is constituted of an anchor segment which interacts with the dispersed particles and a tail segment, which extends into the solution and are able to deposit onto the O/W interface and reduce interfacial tension, protecting oil droplets against aggregation (Woodard and Jasman, 1985).

Table 3 presents the influence of different OEO concentrations on the nanocapsules physiochemical characteristics and EE% while keeping a constant PCL/surfactants ratio. The nanocapsules formation was found to depend on OEO concentrations. Thus, the use of the same concentration of PCL with different OEO concentrations, operating with the same surfactants concentrations and formulation conditions, better results were seen with 1/3.2 ratio of PCL to OEO regarding mean size, PDI, ZP, and EE%. Moreover, good encapsulation efficiencies (EE%) were obtained for all nanocapsules formulations. Although, PCL-OEO-NCs$_1$ presented the most important retention of the essential oil with $85.89\pm2.40\%$, demonstrating the capability of PCL to hold the essential oil within its polymeric matrix and suggesting a high affinity between the hydrophobic polymer and the essential oil molecules.

Overall, the nanoprecipitation method gives good encapsulation efficiencies. Notably, during the preparation of PCL-OEO-NCs$_2$ and PCL-OEO-NCs$_3$, the milky suspension was obtained with an excess of oil droplets which explains the lower EE%. Indeed, the increase of PCL amount to the amount of oregano essential oil resulted in nanocapsules with a smaller size, good PDI and higher zeta potential (Ephrem et al., 2014). Consequently, the best suspension of nanocapsules in terms of a mean size, PDI and ZP have been obtained with a 1/3.2 mass ratio of PCL/OEO. The optimized preparation PCL-OEO-NCs$_1$ was, thereafter, selected for further experiments since it presented adequate nanotechnological characteristics (size, polydispersity distribution, zeta potential, encapsulation efficiency and morphology) as well as the bioactive compound delivery systems (pH and OEO content).

3.2 Characteristics of PCL-OEO-MSs

The preparation of the microspheres by an oil-in-oil-in-water (O1/O2)/W double emulsion was performed according to Carreras et al. (2013). The microspheres preparation variables and concentration of polymer to OEO ratio were set according to the previously reported Carrera's method carried out in our group. The double emulsion solvent evaporation was prepared by two-step emulsification process involving the mixing of an oil/oil emulsion and forming the O$_1$/O$_2$ phase followed by its emulsification in an aqueous phase. Table 4 states the physicochemical characteristics using multiple techniques outlined in the experimental part. The different process parameters were conducted to produce microspheres suspension with a diameter in the range of 2000 nm and exhibiting a monomodal size distribution. Only two conditions were examined since the desirable size was obtained. In fact, the development of biodegradable polymer microspheres for the controlled-release and efficient delivery applications of natural bioactive compounds is challenging due to the difficulty of specifically designing systems exhibiting precisely controlled release rates. Besides, the preparation of stable and well-defined polymeric particles in terms of size and shape is of interest since it is an important parameter to define the controlled release system over a significant duration of times as well as the form of application of the finished dosage form. The control of PCL microspheres size and distribution may provide an improved methodology to tailor the carvacrol release kinetics from biodegradable-polymer microspheres.

alt-text: Table 4

Table 4

(i) The presentation of Tables and the formatting of text in the online proof do not match the final output, though the data is the same. To preview the actual presentation, view the Proof.

Experimental results of PCL-OEO-MSs expressed as mean ± SD.

Formulations	PCL/OEO ratio	PS [a] (nm)	PDI [b]	ZP [c] (mV)	EE [d] (%)
PCL-MSs	1/0	1620.00 ± 47.62	0.19 ± 0.05	~~-8.77-0.27~~ −8.77 ± 0.27	−
PCL-OEO-MSs	1/1	1759.00 ± 162.6	0.86 ± 0.23	−15.7 ± 1.56	47.52 ± 0.52

Values are the mean $\pm$ SD.

Notably, the prepared suspension appeared as white and turbid. Regarding the mean particle size results, PCL-MSs showed an average diameter of 1620.00 ± 47.62 nm. Likewise, microspheres of PCL-OEO-MSs were produced with 1759.00 ± 162.6 nm in mean size and presented a macroscopically homogeneous size distribution (Table 4).

Polydispersity index values in the range of 0.19 ± 0.05 were observed for PCL-MSs and 0.9 ± 0.23 were obtained for PCL-OEO-MSs, revealing the heterogeneous distribution of the colloidal suspension loaded oregano essential oil.

Moreover, the PCL microspheres, bearing negative charges, presented negative zeta potential values for the blank microspheres PCL-MSs (~~-8.77-0.27 mV) and (--~~ $-8.77 + 0.27$ mV) and (-15.7 ± 1.56 mV) for PCL-OEO-MSs. As observed, the negative zeta potential values were closed to zero, reflecting a steric stabilization effect.

In fact, the relation between the particle size and the surface charge of the microspheres is of interest. Compared with PCL nanocapsules, the smallest particles acquired a higher negative zeta potential compared with larger particles. Therefore, an increase or a decrease in the surface charged groups will result in a higher or lower zeta potential. The significant increase in the absolute zeta potential value may refer to higher dispersion stability that resulted in a more stable suspension and vice-versa. This reflects the dependency of the zeta potential on the charge density (Holmberg et al., 2013).

In this work, the PVA was added to the aqueous phase in the amount of 2% (w/v) and the microspheres were prepared under this optimum condition. In a recent study, Iqbal et al. (2015) have revealed a significant influence of PVA concentration on the particle size and morphology of polycaprolactone microparticles prepared by double emulsion. Results indicated that by increasing PVA concentration from 0.05 to 0.2%, the particle size decrease and beyond this value, there was no significant effect on mean particle size. Furthermore, the surface of obtained nanoparticles with 0.5% PVA presented a smooth surface with a regular rounded shape and broad size distribution. However, an increase in PVA concentration up to 2–3% has led to a clumping behavior of the particles and this was due to the excessive PVA resulting in sticking of particles during drying. PVA, as an amphipathic polymer, can be considered as a polymeric surfactant that stabilizes microspheres suspensions through the steric effect (Piazzon Tagliari et al., 2015) and the influence of its concentration in the external water phase on the size of resultant microspheres is significant (Maia et al., 2004).

Moreover, this process conditions resulted in good encapsulation efficiency rate of $47.52 \pm 0.5\%$ which could be considered satisfactory, since there have no previous reports in the literature in double emulsion formulations produced based on the use of essential oils. However, ~~de Sousa et al. (2013)~~ [Instruction: Please

efficiency has dramatically decreased when PVA concentration has increased. Such a result was justified with the use of a higher concentration of PVA (2%, w/v) in the external aqueous phase.

3.3 Morphology and surface characteristics

The scanning electron microscopy (SEM) was carried out to visualize the size and the shape of both PCL nanocapsules and microspheres. The particle size estimated by the DLS technique was found to well correlate with the microscopy analysis. It can be inferred from Fig. 2a that the PCL nanocapsules have a spherical shape of the core/shell and a smooth surface nanomorphology and their mean size was found to be nearly 200 nm, where the polymeric shell of PCL surround the oily core with Tween 80 as a stabilizer. In general, the concentration of the polymeric shell is an important parameter influencing the thickness of the nanocapsules membrane. Several studies have admitted that nanocapsules produced with PCL and nanoprecipitation process provide shell thickness values around 10 nm to 20 nm (Cauchetier et al., 2003; Rübe et al., 2005).

Fig. 2

SEM images of (a) PCL-OEO-NCs$_1$ and (b) PCL-OEO-MSs.
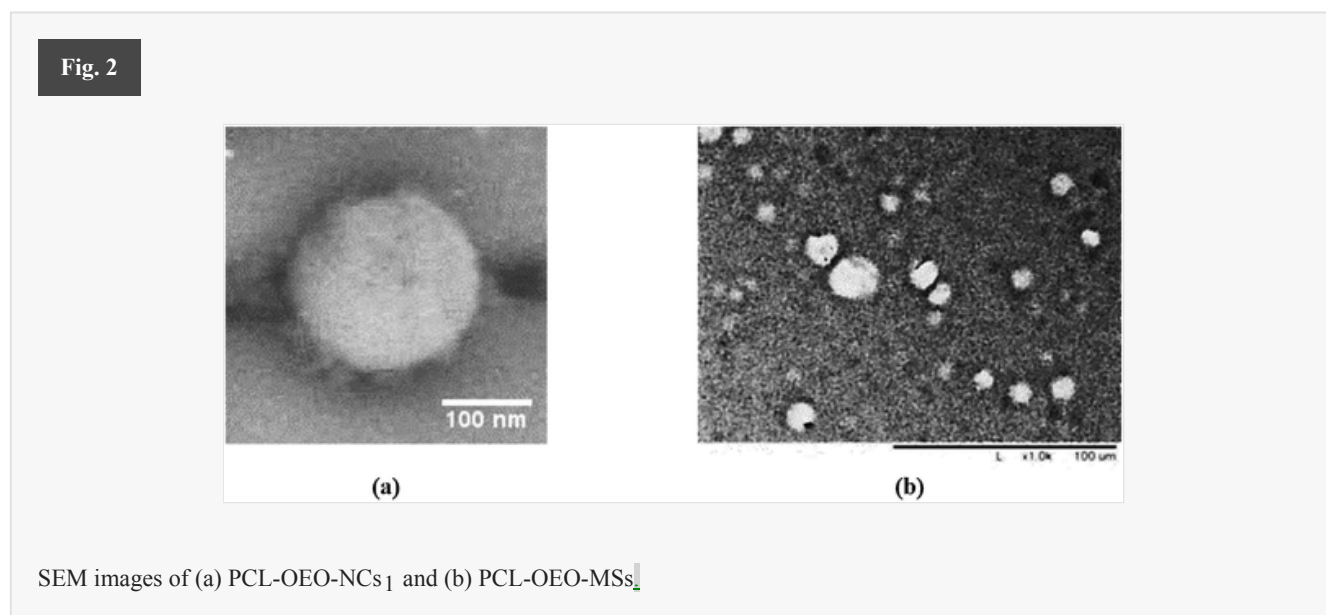
Besides, SEM photomicrograph depicted in Fig. 2b revealed heterogeneous populations of microspheres in the range of 2000 nm in size. Moreover, the porous microspheres were formed as a result of the complete evaporation of the organic solvent (DCM) during the production process (Zhao et al., 2017).(Zhao et al., 2017).

3.4 Thermal analysis

3.4.1 Thermogravimetric analyses (TGA)

Thermogravimetric analyses Fig. 3A and B have been used to evaluate weight losses of the different samples in function of the temperature and to evaluate the thermal stability of the aromatic nanocapsules and microspheres. TGA and DTG thermograms of raw PCL, OEO, PCL-OEO-NCs$_1$, and PCL-OEO-MSs were

determined. The other components were collected as references, revealing the distinct mass losses and indicating thermal decomposition in different stages.
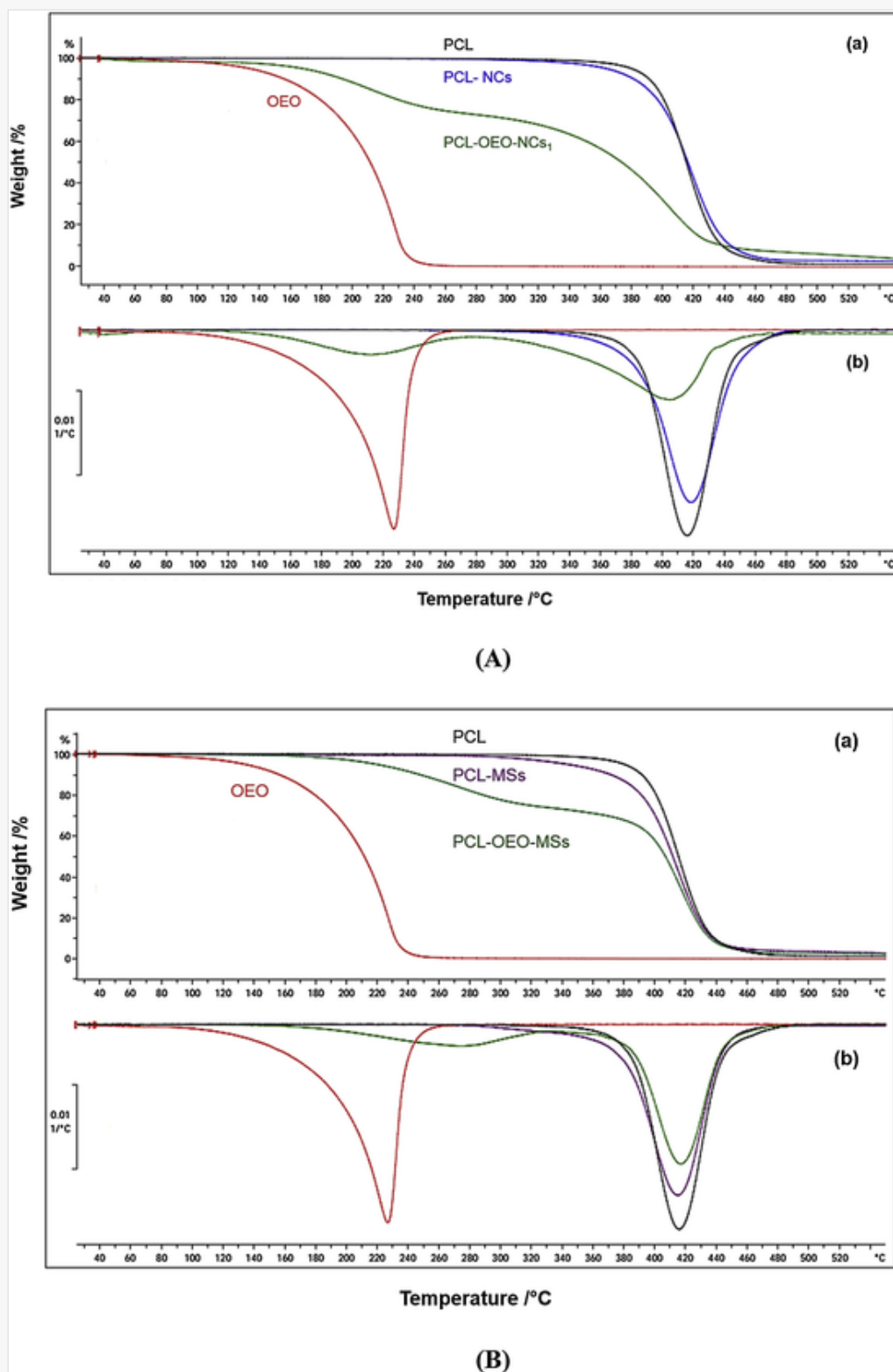
Thermogravimetric curves of (A): (a) PCL, OEO, PCL-OEO-NCs$_1$, PCL-NCs and (b) the first derivatives (DTGA) and of (B): (a) PCL, OEO, PCL-OEO- MSs, PCL-MSs and (b) the first derivatives (DTGA).

The PCL started to degrade slowly after 300 °C and rapidly, reached the decomposition temperature at 414.87 °C, which was due to the complete breakage of the C-C backbone of the PCL chains. Fig. 2 showed that oregano had only one stage in the mass loss which decreased quickly from 140 °C to 240 °C. Therefore, when the temperature reached 250 °C, the weight of essential oil was reduced by 100%.

Unloaded PCL-NCs and PCL-MSs showed one-step mass degradation at around 383.43 °C, due to the onset of degradation in the sample. This behavior was associated with PCL decomposition behavior. In N_2 atmosphere two-stage thermal degradation behavior for PCL-OEO-NCs$_1$ was observed, resulting in two steps in weight loss. The first degradation stage occurred in the range of 95.17 °C–278.65 °C with a 25% weight loss and T_{max1} of 213.67 °C. The mass loss was mainly due to the degradation of OEO, whilst a second degradation stage was attributed to the main degradation of the polymeric matrix PCL, which has appeared at around 278.67 °C–550.36 °C with T_{max2} at 405.34 °C and a total weight loss of 74%. Two peaks were also observed in the DTGA curve of the OEO nanocapsules, one at 215 °C was related to the release of oregano essential oil and the other was recorded at 415 °C and was attributed to the decomposition of the shell material. In the thermogram of PCL-OEO-MSs obtained with double emulsion, two thermal events were also observed. The microspheres showed a mass loss with about 26.64% weight loss and T_{max1} of 273.34 °C and a significant one at around 480 °C with T_{max2} at 415.14 °C and 71% of total weight loss.

Comparing the fusion temperature of OEO to that of loaded nanocapsules, a greater loss in pure compound mass was seen. However, the volatile compound showed a slight loss for nanocapsules which may be due to essential oil adsorbed and blooming the surface. Consequently, OEO encapsulation into the polymeric matrix was found to enhance oil thermal stability. Moreover, no other degradation step was observed, indicating that the water was eliminated during the evaporation process and the surfactants have been completely removed. Therefore, the TGA results confirmed oregano thermal stability and its resistance from loss during the heating process.

3.4.2 Differential scanning calorimetry (DSC)

DSC experiments were performed to investigate the physical state of the OEO encapsulated in the NCs and MSs, as well as the pure OEO and possible polymer interactions. Thermograms of pure PCL, free OEO, PCL nanocapsules and PCL microspheres are presented in Fig. 4A and B and are shown the onset temperature (T_0), the endset temperature (T_f), melting temperatures (T_m) and fusion enthalpy (ΔHm), already summarized in Table 5.

Fig. 4
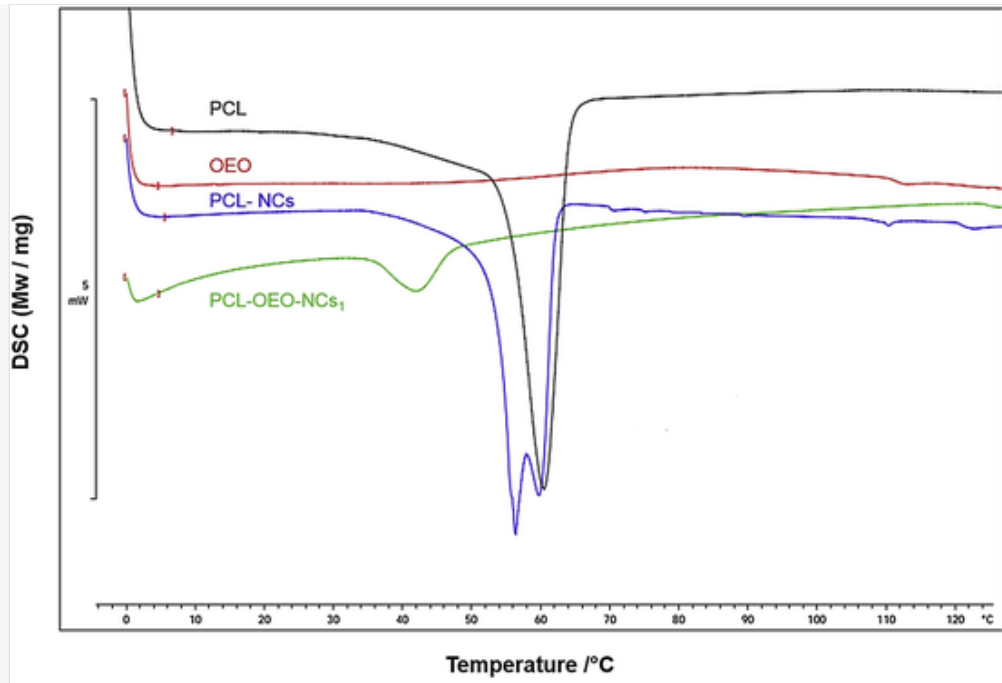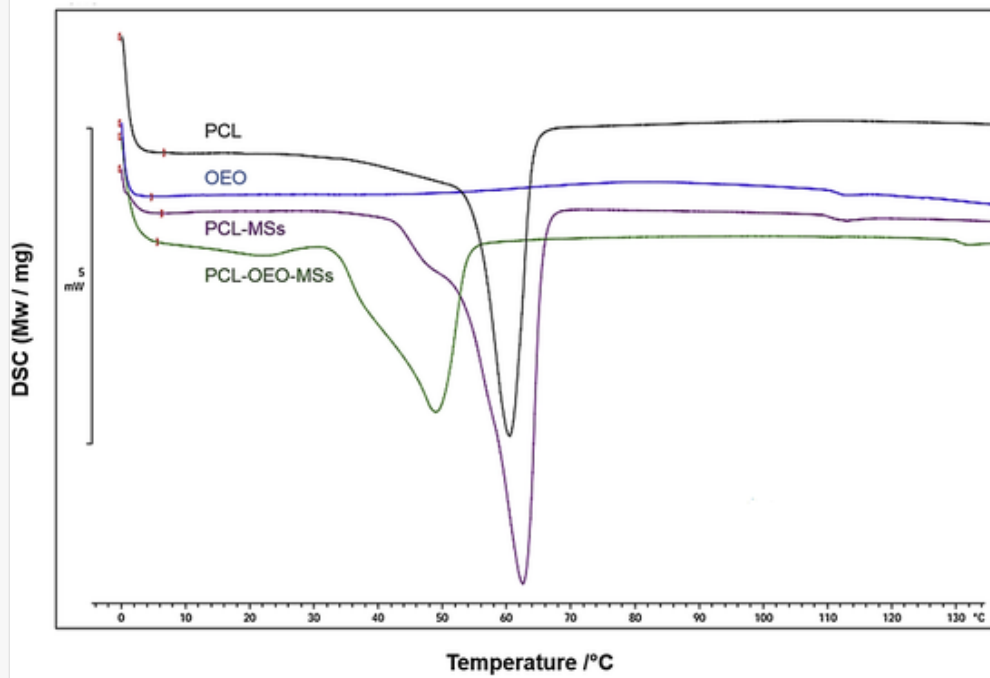
DSC thermograms of (A): PCL-OEO-NCs$_1$, (B): PCL-OEO-MSs and the different components at a heating rate of $10\,°C/min$.

Table 5

Thermal analysis values obtained from DSC thermograms of PCL, OEO, Span 80, Tween 80, PVA, PCL-OEO-NCs$_1$, PCL-NCs, PCL-OEO-MSs, and PCL-MSs.

Samples	T_0 [a] (°C)	T_f [b] (°C)	ΔT $(T_f - T_0)$ [c] (°C)	T_m [d] (°C)	ΔH_m [e] (J/g)
PCL	54.66	64.03	9.37	60.35	77.58
Tween 80	29.67	90.94	61.27	66.62	40.67
Span 80	121.16	130.19	9.03	123.79	1.15
PVA	54.03	132.03	78	93.45	22.99
OEO	11.63	76.07	64.44	45.29	8.68
PCL-OEO-NCs$_1$	35.36	47.21	11.85	42.00	16.23
PCL-NCs (Empty)	53.0649.89	61.6361.99	8.5712.1	56.1859.52	44.7526.97
PCL-OEO-MSs	33.14	53.75	20.61	48.87	54.52
PCL-MSs (Empty)	53.75	65.46	11.71	62.28	84.77

Table Footnotes

[a] ~~onset temperature~~[b]~~final temperature~~[c]~~melting temperature range~~[d]~~melt temperature~~[e]Onset temperature.

Final temperature.

Melting temperature range.

Melt temperature.

~~usion enthalpy.~~Fusion enthalpy.

OEO showed a sharp endothermic event with a wide melting range from 11.63 °C to 76.07 °C ($\Delta T = 64.44$ °C), and a melting temperature (T_m) around 45.29 °C corresponding to its volatilization. The DSC thermogram of PCL presented a melting temperature and ΔH_m value of 60.35 °C and 77.58 J/g, respectively. As can be seen in Fig. 4A, PCL-NCs exhibited the characteristic melting endotherm of PCL with a slight shifting around 59.52 °C (instead of 60.35 °C). Furthermore, PCL-MSs presented a melting temperature value of 62.28 °C related also to the melting temperature of PCL (Fig. 4B). In fact, when PCL dissolved in acetone and, then, precipitated without any oil loading, the melting temperature shifted to low temperatures. This was explained by its rapid precipitation from the solvent which freezes its structure in a less ordered arrangement and accordingly, is responsible for the lower melting temperature compared with the pure PCL (Mossotti et al., 2015). ~~(Mossotti et al., 2015).~~

Furthermore, PCL-OEO-NCs$_1$ thermogram showed a single endothermic peak of the semi-crystalline PCL but was shifted to a lower temperature (42.00 °C). Therewith, in the PCL-OEO-MSs, the melting temperature was found to be reduced by 15 °C lower ($\simeq$ 35 °C), was shifted to a lower temperature (48.87 °C). In fact, the endothermic event corresponding to the glass transition of PCL remained visible for both unloaded and loaded

particles but was shifted to lower temperatures with some broadening of the peak due to the intensified effect in the presence of oregano, corroborating the idea of probably occasioned intermolecular interactions between the oil and the polymer.

In both cases, the disappearance of OEO endothermic peak in this curve indicates that it was dispersed within the polymeric system of the NCs and MSs, either is confined in an oily core and/or adsorbed to the polymer wall (Couvreur et al., 2002). This was also explained with the broadening pic presence which was due to the intensified effect in the presence of higher content of encapsulated oregano. In addition, PCL is a semi-crystalline polymer and its crystallinity tends to decrease with an increase in molecular weight (Kostakova et al., 2017). ~~(Kostakova et al., 2017).~~ Furthermore, the thermal stability of the shell material of the particles was lower than that of empty particles which were due to the plasticization effect of the core material. Thus, the essential oil presence inside the polymeric matrix has possibly promoted changes in its characteristics and so was shifted to smaller temperatures.

3.5 ATR-FTIR analyses

ATR-FTIR spectroscopy analyses were performed to examine the surface chemical structure of the PCL-OEO-NCs and PCL-OEO-MSs and the possible interactions between the essential oil and the polymer forming the particles. FTIR peaks were attributed for stretching and bending vibrations that characterize the functional groups which showed that the particles are functionalized with O─H (Fig. 5).

Fig. 5
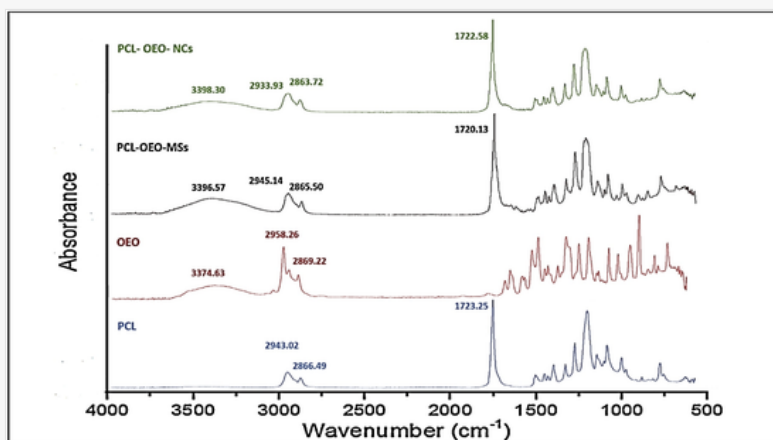
FTIR spectra of (a) raw PCL and (b) OEO, (c) PCL-OEO-NCs, (d) PCL-OEO-MSs.

The PCL spectrum presented a strong characteristic peak at 1723.25 cm^{-1} attributed to the carbonyl-stretching mode C══O. Two vibration bands were observed at 2943.02 cm^{-1} ~~and 2866.49 cm^{-1}~~ and 2866.49 cm^{-1} assigned to asymmetric and symmetric stretching of CH$_2$, respectively. Moreover, the peak at 1294 cm^{-1} was assigned to the backbone C─ ~~C and C~~ C and CO─ stretching modes in the crystalline phase of PCL, whereas the peaks at 1178 cm^{-1} ~~and 1163.8 cm-1 are due to symmetric COC stretching and CO, C~~ and 1163.8 cm^{-1} are

due to symmetric COC stretching and CO, CC —――― stretching in amorphous phase, respectively (Elzein et al., 2004).

Oregano essential oil (OEO) exhibited a broad OH stretching peak at $3374\,cm^{-1}$, attributed to carvacrol. A symmetric and asymmetric stretching peaks CH— were revealed at $2869\,cm^{-1}$, $2926\,cm^{-1}$, and $2958\,cm^{-1}$. In addition, OEO spectra shows peaks at $1589\,cm^{-1}$ (N H bending), $1458\,cm^{-1}$ (CH$_2$ bending), $1253\,cm^{-1}$ (C O C stretching), $1117\,cm^{-1}$ (C O C stretching) and $937\,cm^{-1}$ (C H bending) (Fig. 5) (Valderrama and Rojas De, 2017).

The spectrum of the prepared nanocapsules and microspheres exhibited peaks for both PCL and oregano related absorption bands. However, there was no evidence of new absorption peaks indicating chemical bonds between PCL and the essential oil presence which has possibly promoted changes in the PCL-OEO-NCs and PCL-OEO-MSs characteristics. Therefore, a new large absorption band appeared at $3398.30\,cm^{-1}$ and $3396.53\,cm^{-1}$ in the nanocapsules and microspheres' spectrums, respectively and this was referred to the O—H stretch from the intermolecular/intramolecular hydrogen bonding. Additionally, slight shifts of the carbonyl stretching (C=O band of the PCL) were detected from $1723.25\,cm^{-1}$ to $1722.58\,cm^{-1}$ to $1720.13\,cm^{-1}$ in the case of nanocapsules and microspheres, respectively. This behavior might be explained by the presence of physical interactions between the OEO and the polymeric chains such as hydrogen bonding that has probably weakened the strength of the ester bond present in PCL (Fig. 5).

3.6 Colloidal stability of formulations

Temperature stress study was conducted to investigate the shelf life of the essential oil loaded in PCL polymeric carrier, the recommended storage conditions and the effect of storage temperature (4 °C, 20 °C and 40 °C) on the stability of the formed emulsions (Figs. 6a–d and 7a–d).
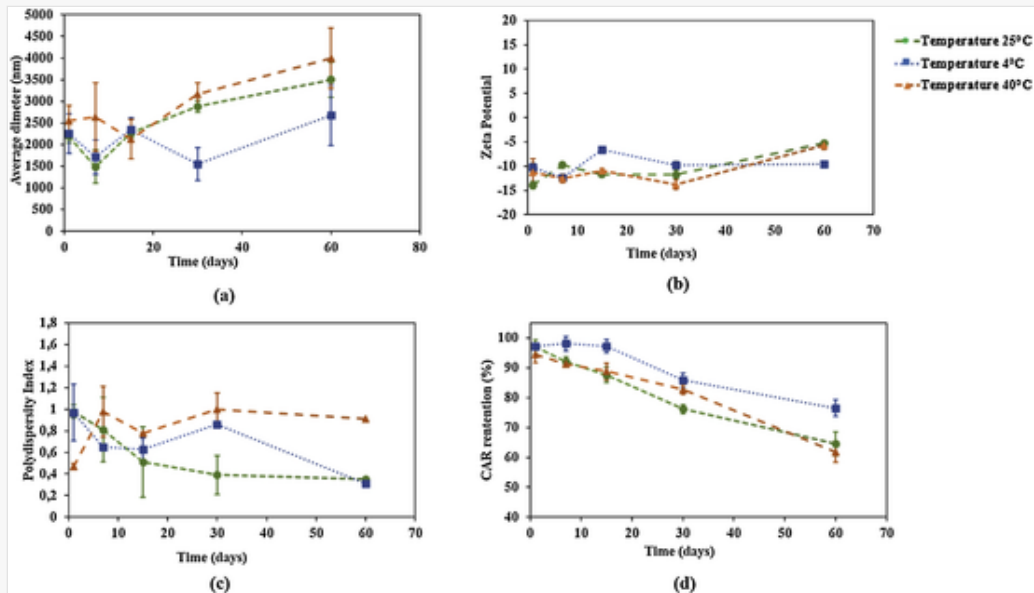

Fig. 6
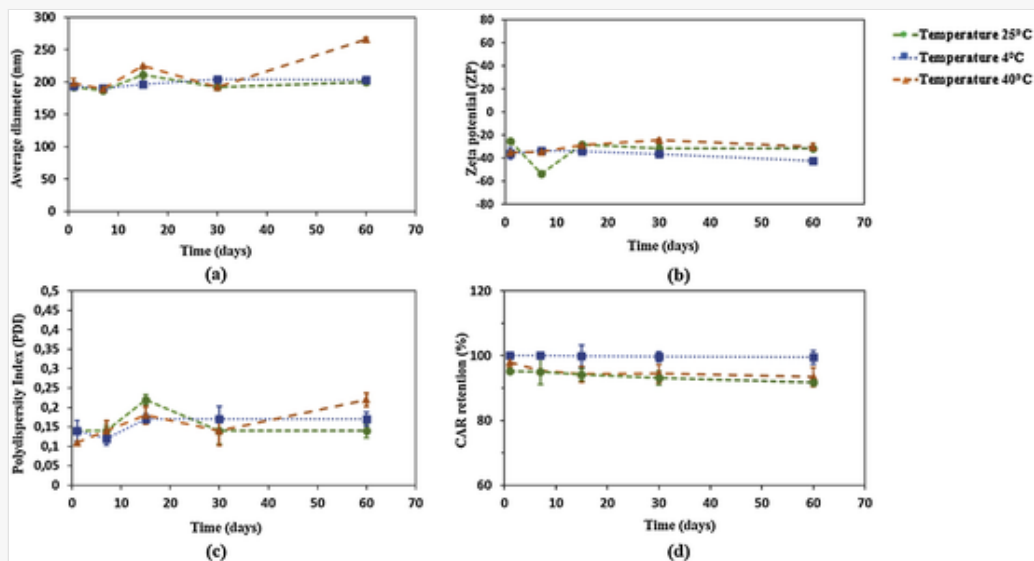
PCL-OEO-NCs$_1$ chemical and physiochemical parameters : (a) average diameter, (b) zeta potential, (c) polydispersity index and (d) CAR retention (%) stored at 4 °C, 25 °C and 40 °C during 60 days-stability test. Standard deviations values are represented by

PCL-OEO-MSs chemical and physiochemical parameters : (a) average diameter, (b) polydispersity index, (c) zeta potential and (d) CAR retention (%) stored at 4 °C, 25 °C and 40 °C during 60 days-stability test. Standard deviations values are represented by bars are not significantly different ($P > 0.05$).

The long-term stability study is an important challenge in improving the stability of either nanocapsules or microspheres that are prone to degradation in the aqueous medium during the storage period. In fact, particles made of biodegradable polymers such as polylactic acid (PLA), polylactic-co-glycolic acid (PLGA), polyglycolic acid (PGA), and polycaprolactone (PCL) are usually prepared as an aqueous dispersion. During their long-term storage, polymer degradation, the bioactive compound leakage, and/ or the bioactive compound degradation may occur in an aqueous environment. These hydrolytically degradable polymers will degrade over time, although at a low rate if the temperature and pH are controlled. Degradation occurs through simple hydrolysis of ester bonds auto-catalyzed by carboxylic groups with an increase in the hydrolysis rate exponentially with degradation time (Hakkarainen et al., 1996). According to França et al. (2016) results, PCL has shown to keep its performance in an aqueous medium, unlike others polyesters which degrade very fast by hydrolyzes reactions, suggesting that PCL products are not prone to rapid hydrolytic degradation and may be projected for use in humid conditions. Macroscopic aspects and homogeneity of the stored samples were discussed. Indeed, no visual modifications have infested the NCs suspensions, such as precipitation, color alteration or phase separation, revealing excellent stability and the homogeneity of the system. However, all MSs samples presented the separation in two phases and the sedimentation of the microspheres. As depicted in Fig. 6, no significant changes were observed in terms of particle size, polydispersity index and zeta potential ($P > 0.05$).

The experimental results, revealed the stability of the OEO nanocapsules suspensions, exhibiting no change in mean droplet diameter and no visible evidence of aggregation or agglomeration occurred, during 60 days of storage at 4 °C. In addition, no marked variation was seen in the particle size diameter profile of nanocapsules stored in water at room temperature as a function of time indicating that the nanotechnological properties were maintained during storage. However, minor changes in nanocapsules size were observed at 40 °C at the end of storage. Accordingly, the formulation was considered physically stable. In addition, the polydispersity index remained stable (in the range from 0.1 to 0.2) indicating the presence of uniform and narrow particles and the absence of agglomerates. In fact, the possibility to obtain aggregated suspension is possible after extended periods of storage in an aqueous environment and such changes could significantly affect the structural integrity of the samples during the storage period.

In the case of microspheres, the physiochemical findings (DLS) presented no significant changes ($P > 0.05$) in Fig. 7a of the sample stored in suspension at 4 °C showed that the colloidal stability was preserved and maintained its initial properties. However, the results depicted in Fig. 7a indicated that samples thermally treated at 25 °C and 40 °C were have shown an enlarging in the particles size. In both cases, the microspheres' size has rapidly increased to nearly double the initial size reaching around 3000 nm upon 1-day storage at 40 °C, and remained unstable thereafter, up to 60 days of storage. Notably, at these temperatures range, phase separation and sedimentation were observed and the mean size increased continuously throughout the storage time investigated. Furthermore, the suspensions polydispersity was affected presenting high mean values > 0.2. According to these observations, the double emulsion was accompanied with the aggregation of microspheres due to the uneven and small sizes showing a bimodal size distribution, and resulted in microspheres sedimentation due to the aggregation of the growing particles. In fact, high polydispersity index values indicate large variations in the particle size by provoking particles aggregation, whereas polydispersity index values smaller than 0.2 suggest that particles are monodisperse (Danaei et al., 2018).

With reference to Mora-Huertas et al. (2010), the zeta potential behavior reflects the surface potential of the nanoparticles and can be influenced by changes in the interface of the nanosystem induced by the dispersant medium: such changes are dependant on the chemical nature of the polymer and related to the stabilizing agent and/or the pH of the solution. The stability of the nanoparticulate systems, resulting nanoprecipitation process, depends on the use of a high hydrophilic-lipophilic balance (HLB) surfactants (Ephrem et al., 2014). The Tween®80 is responsible for preventing and/or reducing particle coalescence rate and the diffusion of the encapsulated active substance. While, the Span®80, which is present in the organic phase, is necessary to obtain a population of nanocapsules with a small and homogeneous size (Khayata et al., 2012). In our case, the freshly prepared nanocapsules suspension presented a highly negative zeta potential (−35 mV). During 60 days of storage, no significant changes were observed with the suspension stabilized with polysorbate 80 at 4 °C reaching −39 mV which presented longer stability as compared with those kept at 25 °C and 40 °C without significant particle size changes during the comparable storage time ($P > 0.05$). This intense charge found on the surface increases the charge-charge repulsions between the nanocapsules, thus, maintaining the colloidal stability of the suspension. On the other hand, the nanosuspensions kept at high temperatures (25 ~~C and 40~~ °C and 40 °C) have shown some changes. Notably, the zeta potential values of the sample stored at 40°C diminished with time and reached a value of -28 mV, which could be explained either the hydrolysis of the PCL polymer and a consequent release of carboxylic groups or may exhibited signs of aggregation due to the

attraction between opposite charges that are evenly distributed in the suspension. Otherwise, an increase in negative zeta values was noticed with samples stored at 25 °C after one week reaching −52 mV. However, in the following days, the zeta potential resumes the starting values and remain stable until the end of the storage. However, the zeta potential values were critical for all the microspheres stored samples. At 4 °C, the curve presented a slight decrease in ZP values and remain stable ($P > 0.05$). In general, a lower zeta potential value indicates colloid instability, which could lead to aggregation of the particles. Therefore, at 25 °C and 40 °C, zeta potential values presented a decrease in the negative zeta potential values towards zero, which is in concordance with the microspheres suspensions behavior revealing an associated aggregation phenomenon. In general, an emulsion may become unstable due to a number of different types of physical and chemical processes. Physical instability results in an alteration in the spatial distribution or structural organization of the molecules (creaming, flocculation, coalescence, partial coalescence, phase inversion, and Ostwald ripening), whereas chemical instability results in an alteration in the chemical structure of the molecules (oxidation and hydrolysis). These mechanisms of emulsion instability may be verified by an increase in mean particle diameter because the particles are in continual motion and collide with one another under normal conditions. The bigger size distribution of microspheres obtained after 60 days of storage could be due to PVA concentration applied during the microspheres production process. During storage, PVA plays an important role in maintaining the stability of the microspheres suspension. Besides, PVA will be adsorbing at both phase interfaces and stabilize the emulsion *via* a steric hindrance effect. So it is still important to understand the aggregation phenomenon occurred during storage and the particles growth step. In fact, during the preparation process, the microspheres were covered by PVA by steric stabilization and were stable. Within the storage period, the nonadsorbed PVA molecules have led to a depletion attraction, which gave rise to depletion flocculation. Withal, the magnitude of depletion attraction is proportional to the osmotic pressure in the aqueous phase which leads to increased particle size and instability (Jenkins and Snowden, 1996).

Fig. 6d presented the ability of the nanocapsules to retain the carvacrol (CAR%) in function of time and temperature. EE% was about 86% and LC% was 6%. (CAR%) retention appeared, thereby, to be compromised by temperature during storage. The results depicted in Fig. 6d showed high retention of carvacrol from all samples kept at different temperatures after 1 day of storage. Lowering the temperature to 4 °C was found to maintain the carvacrol retention capacity up to 15 days and showed longer stability compared with other temperatures. During the following days, the nanocapsules suspension maintained its homogeneity and its opacity. However, carvacrol retention decreased after 30 days to (99.86%) and remained stable up to 60 days of storage (99.5%). Besides, the higher temperatures have influenced the emulsion kept at 25 °C and 40 °C and an oiling-off was presented after 60 days of storage in both samples with 91.79% and 93.4% decrease, respectively. As previously mentioned, the stability of the colloidal nanosuspensions was favored by electrostatic repulsion effect, which prevents aggregations and collisions between the fine nanocapsules. The electrostatic effect was also confirmed by the highly negative zeta potential values due to repulsion among similar charges which contributed also to lower carvacrol leakage from the PCL polymeric shell.

During the course of 60 days of storage, the microspheres suspensions presented a significant decline of carvacrol retention (CAR%) (Fig. 7d), indicating oil leakage (surface desorption and/or diffusion to the aqueous medium). This kinetic could be attributed to the oil incorporation pattern, wherein the PCL microspheres, the oil is more adsorbed onto the particle surface. In such cases, when hydrophilic molecules are

encapsulated using the double emulsion solvent evaporation method with hydrophobic polymers such as PCL, the hydrophilic molecules are adsorbed near the surface of microspheres, showing a burst effect. Therefore, the initial oil released from microspheres could be due to oregano adsorption on the microspheres' surface, which releases when it comes into contact with dissolution medium. Further, the results depicted in Fig. 7d revealed that microspheres stored at $4\,°C$ had a high CAR retention capacity up to 15 days in comparison to samples stored at $25\,°C$ and $40\,°C$. In particular, for samples kept at $25\,°C$ and $40\,°C$ a decrease in CAR retention (%) was observed from the first months reaching 76.20% and 82.70%, respectively. Following the second month, the retention in carvacrol dropped to 64.56% and to 61.84% for samples stored at $25\,°C$ and $40\,°C$, respectively. The aggregation and/or fusion whereof results have depicted could be the leading cause of their increase in the carvacrol leakage during storage.

The physicochemical properties of the prepared suspensions revealed the stability of the system based on the oil and the polymer phase, the surfactants nature and the chemical process. Consequently, the formulations system formation has a considerable impact on emulsions stability. Results confirmed that time and temperature didn't significantly influence the physicochemical properties of suspensions stored at $4\,°C$ and $25\,°C$ and the emulsion remained stable over 60 days. Moreover, data showed that the low storage temperature of $4\,°C$ is more efficient to effectively preserve the carvacrol in the PCL polymeric carrier with a nearly complete recovery of carvacrol. In addition, there was no shift of retention time for the carvacrol peak in the HPLC profile, confirming no structural change of the carvacrol after encapsulation.

3.7 pH stability

The chemical stability of the suspension samples, stored in the water medium, was evaluated by the determination of the pH, concomitant to the morphological features of the particles and the carvacrol encapsulation content. In fact, results can predict the chemical stability of the polymeric shell, since a change in the pH indicates its stability or its degradation in the polymeric solution (Grillo et al., 2011). Thus, the influence of the storage temperature on the evolution of pH as a function of time was discussed. Results from nanocapsules samples indicate that the pH was slightly influenced by storage conditions since the formulations did not present major alterations during 60 days of storage ($P > 0.05$). The mean diameter of the nanocapsules was, consequently, not altered indicating that the electrostatic repulsion maintained the colloidal physical stability. On the other side, pH change may present a considerable effect on the zeta potential of the stored nanocapsules when the time and temperature of storage are varied. As mentioned earlier, the pH of the bulk solution can influence the zeta potential and, consequently, can alter the physical stability of the nanosystems (Mora-Huertas et al., 2010; Singh et al., 2009).

Immediately after preparation, the PCL-OEO-NCs$_1$ presented an initial pH value of 4.92 ± 0.01. The cold storage of the nanocapsules maintained close pH values, showing no significant change in the pH values ($P > 0.05$), revealing excellent stability during the study period (Table 6). In accordance with Fig. 6b, it was observed that the nanocapsules zeta potential values were experimentally constant. In this stored sample, stability was due to the strongly negative-charged zeta potential and the lack of agglomeration (Berg et al., 2009). On the contrary, the higher temperatures induced changes in the pH of the colloidal dispersions. PCL nanoparticles kept at $25\,°C$, showed a decrease in pH values that varied from 4.92 ± 0.01 to 3.82 ± 0.05.

Concurrently, the nanocapsules demonstrated a slight increase in the zeta potential towards negative values, reaching ($-52\,$mV) over a one-week time course, and then, took the initial state to remain stable during the end of the storage period. The sample stored at $40\,°$C, showed a slight decrease in the zeta potential values and reached a pH value of 3.94 ± 0.15 after 60 days of storage. However, this decrease still led to a very negative zeta potential of $-28\,$mV, a number commonly used to indicate the solution stability by electrostatic repulsion.

Besides, pH results of microspheres showed an initial pH value of 5.98 ± 0.02. The evaluation of the chemical stability of the PCL microspheres showed significant pH changes, as a function of time and temperature. Indeed, samples stored at $25\,°$C and $40\,°$C presented lower pH values of 4.35 ± 0.18 and 3.32 ± 0.02, respectively, after 60 days of storage when compared with the sample stored at $4\,°$C which presented a pH value of 5.03 ± 0.11. These findings admitted that changes in the pH medium can be explained by the presence of oregano oil in the organic phase with the microspheres agglomeration which resulted in the concomitant release of the oil into the surrounding medium. Overall, the changes occurred in pH values during 60 days were not significant ($P>0.05$) and since, this decrease to low pH values (<4.0) may be prompted by the PCL degradation which was due to the enhanced relaxation of its chains and the release of its acidic functional groups, as it was explained in earlier studies (Labet and Thielemans, 2009; Persenaire et al., 2001).Olivier Persenaire et al., 2001). Such decrease was mostly referred to the poly-ε-caprolactone biodegradation, because of the susceptibility of its aliphatic ester linkage to hydrolysis and the formation of free radicals, along with the high surface area of the nanocapsules, and also with the presence of oxygen in the vials. The acidic pH generates, as a result, higher negative charges on the surface as proved with the negatively recorded zeta potential values. However, the rate of PCL hydrolysis can be accelerated causing unstable suspensions and visible sediments in sample vials. Nonetheless, no visible sediment altered the nano-suspensions formation before or during the storage period was conducted revealing the stability of the nano-formulations, which was also confirmed by the zeta potential (ZP) values (Table 6).

alt-text: Table 6

Table 6

> The presentation of Tables and the formatting of text in the online proof do not match the final output, though the data is the same. To preview the actual presentation, view the Proof.

The effect of storage time (1, 7, 15, 30, 60 days) and temperature on pH of nanocapsules (PCL-OEO-NCs $_1$) and microspheres (PCL-OEO-MSs). Mean $\pm$ standard deviation values.

	Formulations					
Storage time (days)	PCL-OEO-NCs $_1$			PCL-OEO-MSs		
	25C4C40C25C4C40°C	4°C	40°C	25°C	4°C	40°C
1	4.83 ± 0.03	5.08 ± 0.16	4.85 ± 0.02	5.68 ± 0.03	5.96 ± 0.01	5.63 ± 0.06
7	4.65 ± 0.01	4.96 ± 0.07	4.69 ± 0.09	5.23 ± 0.04	6.08 ± 0.03	5.19 ± 0.08
15	4.40 ± 0.07	4.82 ± 0.03	4.43 ± 0.18	4.84 ± 0.01	5.78 ± 0.14	4.64 ± 0.23

30	4.16 ± 0.12		4.65 ± 0.14	4.21 ± 0.06	4.65 ± 0.02	5.61 ± 0.08	4.26 ± 0.04
60	3.82 ± 0.05		4.51 ± 0.02	3.94 ± 0.15	4.32 ± 0.18	5.03 ± 0.11	3.32 ± 0.02

Mean ± standard deviation values are not significantly different ($P > 0.05$).

However, sediments were notably obtained with all microspheres samples during the storage period revealing the nonstability of this nanosystem in the water medium. We can conclude that pH changes had a considerable effect on the stability state of the oregano nanocapsules or microspheres when monitoring the time and temperatures, which reveal the stability or the nonstability of the nano-formulations.

3.8 Multivariate data analysis

The preceding study of the long-term storage stability, with time-temperature monitoring, highlighted the impact of selected controllable factors on the stability of the two studied systems in terms of physicochemical parameters. A principal component analysis (PCA) was performed, considering the simultaneous action of all of the analyzed variables and their relationship with storage factors (storage time and temperature). In the following text, these abbreviations were used: particle size (PS), polydispersity index (PDI), zeta potential (ZP), carvacrol retention (CAR%) and pH values (pH). Each sample on the graph was described as follows: name of the system-temperature-time.

According to Table 7 and Fig. 8, the first two PCAs factors accounted for 90.05% of the total variability of the data and were selected for a PCA graphical representation. The scores and correlation loadings from the first and second principal components (PC1 and PC2) are stated in Fig. 9.

alt-text: Table 7

Table 7

> ⓘ The presentation of Tables and the formatting of text in the online proof do not match the final output, though the data is the same. To preview the actual presentation, view the Proof.
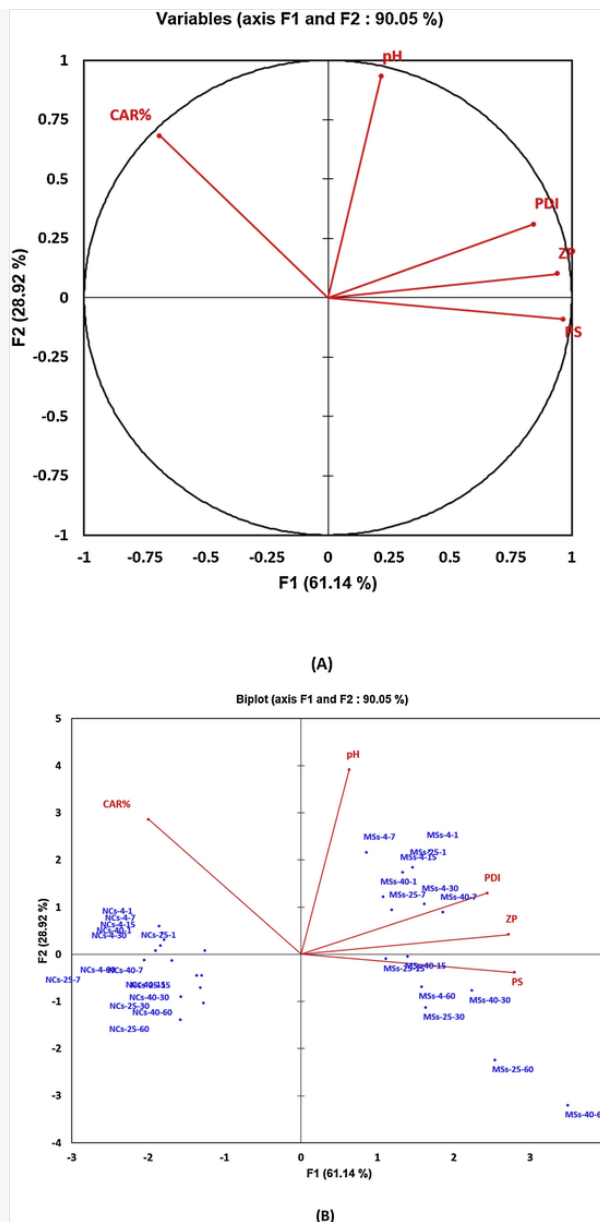
Eigenanalysis of the covariance matrix.

	F1	F2	F3	F4	F5
Eigenvalue	3.057	1.446	0.306	0.134	0.057
Variance (%)	61.137	28.916	6.128	2.679	1.140
Cumulative (%)	61.137	90.053	96.181	98.860	100.000

Fig. 8
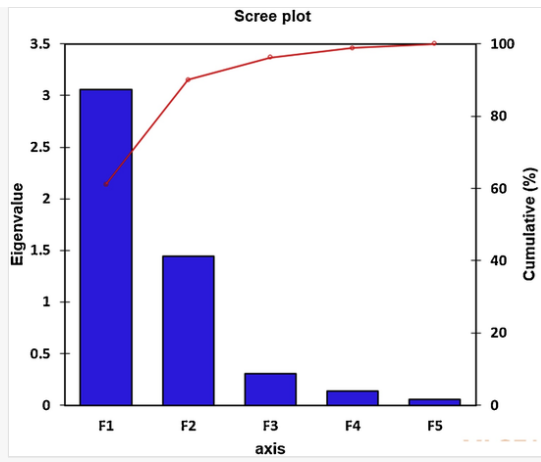
Scree plot for PCA.

Fig. 9

Score plot and correlation loading plot from PC1, PC2 (A and B) from the principal components analysis (PCA) of colloidal nanocapsules and microspheres (PCL-OEO-NCs and PCL-OEO-MSs). All samples and analytical parameters were used. NCs indicates nanocapsules formulation, and MSs indicates microspheres formulations; 4, 25 and 40 in the samples' description refer to the storage temperature (°C). The last number of the sample description indicates the storage time (days).

The first principal component PC1, accounting for 61.14% of the total variation, described the differences in physicochemical properties (PS, PDI, and ZP) of the colloidal systems as affected by storage factors (temperature and time). The second principal component PC2, representing 28.92% of the total variation, described mainly the effect of storage conditions on pH variation as well as the carvacrol content (CAR%) variation. In one hand, PC1 separated the colloidal systems according to their physicochemical properties (PS, ZP, and PDI) which appear correlated positively to PC1, particularly their particle size (PS) showing a high correlation to the component ($R=0.967$). The zeta potential score was also positively correlated to this PC ($R=0.941$), as well as the PDI ($R=0.843$). Moreover, PS, PDI, and ZP were depicted together and in the same direction. Secondly, PS and ZP are closely coupled. These relationships were confirmed by Pearson correlation

coefficients which measures the strength of the association between two variables, where PS score was positively correlated to the ZP ($r=0.866$, $p < 0.0001$), positively correlated to PDI ($r=0.753$, $p < 0.0001$) and PDI was positively correlated to ZP ($r=0.756$, $p < 0.0001$). These results confirm an important relationship and imply the high correlation between the three variables. Conversely, PC2 driven by the differences in the aqueous storage medium, showed a positive correlation with pH ($R = 0.932$) as well as the carvacrol content (CAR%), as shown by its correlation to this PC ($R=0.681$). This PC was also negatively correlated to the PS score ($R= -0.092$).

From the correlation circle (Fig. 9A), the obtained PCAs showed the presence of two mainly clustered groups. One group related to microspheres was situated in the right region of the plot.

Whereas, the nanocapsules group were located on the opposite side of the plot. This shows that groups were mainly discriminated based firstly on their colloidal system type. Furthermore, samples were also regrouped in the function of their temperature and storage days where storage days and temperature influence were significant. Notably, samples stored at cold temperature during the first 15 days were located in the upper part of the plot while those related to higher storage temperature and stored up to 30 and 60 days were located at the lower region of this graph. From the depicted results cited above, a first statement leads to conclude that the most highly significant factor influencing the stability of systems is the temperature. According to Fig. 9B, it has been shown that stored microspheres at 25°C –40°C exhibited a larger particle size with lower carvacrol retention (CAR%). Their percentages decreased considerably over storage time and temperature. This relationship was confirmed by Pearson correlation coefficients, where the PS score was negatively correlated to the carvacrol retention (CAR%) ($r = -0.734$, $p < 0.0001$). In contrary, nanocapsules samples characterized by low PS and PDI values exhibited high retention of CAR% regardless of the change of temperature and storage time. This important difference was observed at the end of storage time between both systems obtained by different preparation methods. Besides, pH results matched the previous findings. pH appeared to correlate with ZP. Therefore, the changes in pH medium presented a considerable effect on the physiochemical parameters, particularly on the zeta potential of the stored samples when the time and temperature of storage are varied.

In conclusion, significant changes between nanocapsules and microspheres stored at different temperatures occurred after 15 days of storage up to 60 days of storage. More carvacrol content loss (CAR%) was observed for both colloidal systems stored at 25°C and 40°C compared with those stored at 4°C.

4 Conclusion

This study examined the successful preparation of oregano-based polycaprolactone particles with different morphologies through nanoprecipitation and double emulsion processes. Uniform spherical nanocapsules were first prepared with good characteristics of particle size distribution PDI (< 0.2) and high encapsulation efficiencies ranging between $50.36 \pm 1.86\%$ and $85.89 \pm 2.40\%$. Withal, the double emulsion method resulted in microspheres of 2000 nm in average size, and considerable oregano essential oil entrapment efficiency. The physicochemical properties were found to be influenced significantly by the encapsulation process. Principal components study demonstrated the relevance of temperature and time factors in maintaining the colloidal systems stability. The stability data indicated that nanocapsules promoted higher carvacrol protection

(99.5±2.09%) at 4 °C and accounted for 93.40±0.11% and 91.79±2.98% at 25 °C and 40 °C, respectively and presented good suspension in water. When comparing the microspheres residual content of carvacrol, only 76.51±2.72%, 64.56±3.98% and 61.84±3.50% were retained after 60 days of storage at 4 °C, 25 °C and 40 °C, respectively. This indicates that nanoencapsulation is highly effective in inhibiting carvacrol loss during storage at 4––40 °C, although, the decrease in carvacrol content has also been demonstrated in environmental conditions 25––40 °C.

These characteristics imply that our investigation provides valuable results for producing stable systems with significant carvacrol retention capability. Nanocapsules might be an interesting strategy to improve the stability and bioavailability of the carvacrol.

Acknowledgments

References

> ⓘ The corrections made in this section will be reviewed and approved by journal production editor.

Adebayo, O., Dang, T., Bélanger, A., Khanizadeh, S., 2013. Antifungal studies of selected essential oils and a commercial formulation against Botrytis cinereaAntifungal studies of selected essential oils and a commercial formulation against *Botrytis cinerea*. J. Food Res. 2, 217–226. doi:10.5539/jfr.v2n1p217.

Almeida, A.P., Rodríguez-Rojo, S., Serra, A.T., Vila-Real, H., Simplicio, A.L., Delgadilho, I., Beirão da Costa, S., Beirão da Costa, L., Nogueira, I.D., Duarte, C.M.M., 2013. Microencapsulation of oregano essential oil in starch-based materials using supercritical fluid technology. Innov. Food Sci. Emerg. Technol. 20, 140–145. doi:10.1016/J.IFSET.2013.07.009.

Atul Bhattaram, V., Graefe, U., Kohlert, C., Veit, M., Derendorf, H., 2002. Pharmacokinetics and bioavailability of herbal medicinal products. Phytomedicine 9, 1–33. doi:10.1078/1433-187X-00210.

El Babili, F., Bouajila, J., Souchard, J.P., Bertrand, C., Bellvert, F., Fouraste, I., Moulis, C., Valentin, A., 2011. Oregano: chemical analysis and evaluation of its antimalarial, antioxidant, and cytotoxic activities. J. Food Sci. 76, C512–C518. doi:10.1111/j.1750-3841.2011.02109.x.

Badri, W., El Asbahani, A., Miladi, K., Baraket, A., Agusti, G., Nazari, Q.A., Errachid, A., Fessi, H., Elaissari, A., 2018. Poly (ε-caprolactone) nanoparticles loaded with indomethacin and *Nigella sativa* L.

essential oil for the topical treatment of inflammation. J. Drug Deliv. Sci. Technol. 46, 234–242. doi:10.1016/j.jddst.2018.05.022.

Baek, J.-S., Choo, C.C., Qian, C., Tan, N.S., Shen, Z., Loo, S.C.J., 2016. Multi-drug-loaded microcapsules with controlled release for management of parkinson's disease. Small 12, 3712–3722. doi:10.1002/smll.201600067.

Beirão-da-Costa, S., Duarte, C., Bourbon, A.I., Pinheiro, A.C., Januário, M.I.N., Vicente, A.A., Beirão-da-Costa, M.L., Delgadillo, I., 2013. Inulin potential for encapsulation and controlled delivery of oregano essential oil. Food Hydrocoll. 33, 199–206. doi:10.1016/J.FOODHYD.2013.03.009.

Beirão da Costa, S., Duarte, C., Bourbon, A.I., Pinheiro, A.C., Serra, A.T., Moldão Martins, M., Nunes Januário, M.I., Vicente, A.A., Delgadillo, I., Duarte, C., Beirão da Costa, M.L., 2012. Effect of the matrix system in the delivery and *in vitro* bioactivity of microencapsulated oregano essential oil. J. Food Eng. 110, 190–199. doi:10.1016/J.JFOODENG.2011.05.043.

Berg, J.M., Romoser, A., Banerjee, N., Zebda, R., Sayes, C.M., 2009. The relationship between pH and zeta potential of ~ 30 nm metal oxide nanoparticle suspensions relevant to *in vitro* toxicological evaluations. Nanotoxicology 3, 276–283. doi:10.3109/17435390903276941.

Bhattacharjee, S., 2016. ~~DLS and zeta potential — What they are and what they are not?~~DLS and zeta potential – what they are and what they are not? J. Control. Release 235, 337–351. doi:10.1016/J.JCONREL.2016.06.017.

Bilia, A.R., Guccione, C., Isacchi, B., Righeschi, C., Firenzuoli, F., Bergonzi, M.C., 2014. Essential oils loaded in nanosystems: a developing strategy for a successful therapeutic approach. ~~Evid. Based. Complement. Alternat. Med.~~Evid. Complement. Alternat. Med. 2014, 1–14. doi:10.1155/2014/651593, 651593.

Božik, M., Nový, P., Klouček, P., 2017. Chemical composition and antimicrobial activity of cinnamon, thyme, oregano and clove essential oils against plant pathogenic bacteria. Acta Univ. Agric. Silvic. Mendelianae Brun. 65, 1129–1134. doi:10.11118/actaun201765041129.

Camele, I., Altieri, L., De Martino, L., De Feo, V., Mancini, E., Rana, G.L., 2012. *In vitro* control of post-harvest fruit rot fungi by some plant essential oil components. Int. J. Mol. Sci. 13, 2290–2300. doi:10.3390/ijms13022290.

Carreras, N., Acuña, V., Martí, M., Lis, M.J., 2013. Drug release system of ibuprofen in PCL-microspheres. Colloid Polym. Sci. 291, 157–165. doi:10.1007/s00396-012-2768-x.

Casanova, F., Santos, L., 2016. Encapsulation of cosmetic active ingredients for topical application – a review. J. Microencapsul. 33, 1–17. doi:10.3109/02652048.2015.1115900.

Cauchetier, E., Deniau, M., Fessi, H., Astier, A., Paul, M., 2003. Atovaquone-loaded nanocapsules: influence of the nature of the polymer on their *in vitro* characteristics. Int. J. Pharm. 250, 273–281.

doi:10.1016/S0378-5173(02)00556-2.

Cerkez, I., Sezer, A., Bhullar, S.K., 2017. Fabrication and characterization of electrospun poly(e-caprolactone) fibrous membrane with antibacterial functionality. R. Soc. Open Sci. 4. doi:10.1098/rsos.160911, 160911.

Çırpanlı, Y., Allard, E., Passirani, C., Bilensoy, E., Lemaire, L., Çalış, S., Benoit, J.-P., 2011. Antitumoral activity of camptothecin-loaded nanoparticles in 9L rat glioma model. Int. J. Pharm. 403, 201–206. doi:10.1016/J.IJPHARM.2010.10.015.

Couvreur, P., Barratt, G., Fattal, E., Legrand, P., Vauthier, C., 2002. Nanocapsule technology: a review. Crit. Rev. Ther. Drug Carrier Syst. 19, 99–134.

Danaei, M., Dehghankhold, M., Ataei, S., Hasanzadeh Davarani, F., Javanmard, R., Dokhani, A., Khorasani, S., Mozafari, M., 2018. Impact of particle size and polydispersity index on the clinical applications of lipidic nanocarrier systems. Pharmaceutics 10, 57. doi:10.3390/pharmaceutics10020057.

de Matos, S.P., Teixeira, H.F., de Lima, Á.N., Veiga-Junior, V.F., Koester, L.S., 2019. Essential oils and isolated terpenes in nanosystems designed for topical administration: a review. Biomolecules 9, 138. doi:10.3390/biom9040138.

Dhivya, S., Padma, V.V., Santhini, E., 2015. Wound dressings - a review. BioMedicine 5, 22. doi:10.7603/s40681-015-0022-9.

Ekor, M., 2014. The growing use of herbal medicines: issues relating to adverse reactions and challenges in monitoring safety. Front. Pharmacol. 4, 177. doi:10.3389/fphar.2013.00177.

Elshafie, H., Armentano, M., Carmosino, M., Bufo, S., De Feo, V., Camele, I., 2017. Cytotoxic activity of *Origanum vulgare* L. on hepatocellular carcinoma cell line HepG2 and evaluation of its biological activity. Molecules 22, 1435. doi:10.3390/molecules22091435.

Elshafie, H.S., Camele, I., 2016. ~~Investigating the effects of plant essential oils on post-harvest fruit decay, in: Fungal Pathogenicity~~Investigating the Effects of Plant Essential Oils on Post-harvest Fruit Decay, in: Fungal Pathogenicity, InTech. doi:10.5772/62568.

Elshafie, H.S., Mancini, E., Sakr, S., De Martino, L., Mattia, C.A., De Feo, V., Camele, I., 2015. Antifungal activity of some constituents of *Origanum vulgare* L. essential oil against postharvest disease of peach fruit. J. Med. Food 18, 929–934. doi:10.1089/jmf.2014.0167.

Elzein, T., Nasser-Eddine, M., Delaite, C., Bistac, S., Dumas, P., 2004. FTIR study of polycaprolactone chain organization at interfaces. J. Colloid Interface Sci. 273, 381–387. doi:10.1016/J.JCIS.2004.02.001.

Ephrem, E., Greige-Gerges, H., Fessi, H., Charcosset, C., 2014. Optimisation of rosemary oil encapsulation in polycaprolactone and scale-up of the process. J. Microencapsul. 31, 746–753. doi:10.3109/02652048.2014.918669.

Feng, R., Song, Z., Zhai, G., 2012. Preparation and *in vivo* pharmacokinetics of curcumin-loaded PCL-PEG-PCL triblock copolymeric nanoparticles. ~~Int. J. Nanomedicine~~Int. J. Nanomed. 7, 4089. doi:10.2147/IJN.S33607.

Ferrándiz, M., Capablanca, L., García, D., Bonet, M., 2017. Application of antimicrobial microcapsules on agrotextiles. J. Agric. Chem. Environ. 6, 62–82. doi:10.4236/jacen.2017.61004.

Fessi, H., Puisieux, F., Devissaguet, J.P., Ammoury, N., Benita, S., 1989. Nanocapsule formation by interfacial polymer deposition following solvent displacement. Int. J. Pharm. 55, R1–R4. doi:10.1016/0378-5173(89)90281-0.

França, D.C., Bezerra, E.B., de S. Morais, D.D., Araújo, E.M., Wellen, R.M.R., França, D.C., Bezerra, E.B., de S. Morais, D.D., Araújo, E.M., Wellen, R.M.R., 2016. Hydrolytic and thermal degradation of PCL and PCL/bentonite compounds. Mater. Res. 19, 618–627. doi:10.1590/1980-5373-MR-2015-0797.

Grillo, R., do E.S Pereira, A., de Melo, N.F.S., Porto, R.M., Feitosa, L.O., Tonello, P.S., Filho, N.L.D., Rosa, A.H., Lima, R., Fraceto, L.F., 2011. Controlled release system for ametryn using polymer microspheres: preparation, characterization and release kinetics in water. J. Hazard. Mater. 186, 1645–1651. doi:10.1016/J.JHAZMAT.2010.12.044.

Guimarães, A.G., Oliveira, M.A., Alves, R., dos, S., Menezes, P., dos, P., Serafini, M.R., de Souza Araújo, A.A., Bezerra, D.P., Quintans Júnior, L.J., 2015. Encapsulation of carvacrol, a monoterpene present in the essential oil of oregano, with β-cyclodextrin, improves the pharmacological response on cancer pain experimental protocols. Chem. Biol. Interact. 227, 69–76. doi:10.1016/J.CBI.2014.12.020.

Gupta, B.S., Moghe, A.K., 2013. Nanofiber structures for medical biotextiles. ~~Biotextiles as Med. Implant.~~Biotextiles Med. Implant. 48–90. doi:10.1533/9780857095602.1.48.

Gupta, R., Rai, B., 2017. Effect of size and surface charge of gold nanoparticles on their skin permeability: a molecular dynamics study. Sci. Rep. 7, 45292. doi:10.1038/srep45292.

Hakkarainen, M., Albertsson, A.-C., Karlsson, S., 1996. Weight losses and molecular weight changes correlated with the evolution of hydroxyacids in simulated *in vivo* degradation of homo- and copolymers of PLA and PGA. Polym. Degrad. Stab. 52, 283–291. doi:10.1016/0141-3910(96)00009-2.

Han, X., Parker, T.L., 2017. Anti-inflammatory, tissue remodeling, immunomodulatory, and anticancer activities of oregano (*Origanum vulgare*) essential oil in a human skin disease model. Biochim. Open 4, 73–77. doi:10.1016/J.BIOPEN.2017.02.005.

Hickey, J.W., Santos, J.L., Williford, J.-M., Mao, H.-Q., 2015. Control of polymeric nanoparticle size to improve therapeutic delivery. J. Control. Release 219, 536–547. doi:10.1016/j.jconrel.2015.10.006.

Holmberg, J.P., Ahlberg, E., Bergenholtz, J., Has. sellöv, M., Abbas, Z., 2013. Surface charge and interfacial potential of titanium dioxide nanoparticles: experimental and theoretical investigations. J. Colloid Interface Sci. 407, 168–176. doi:10.1016/J.JCIS.2013.06.015.

Honary, S., Zahir, F., 2013. Effect of zeta potential on the properties of nano-drug delivery systems - a review (Part 1). Trop. J. Pharm. Res. 12, 255–264. doi:10.4314/tjpr.v12i2.19.

Honary, S., Zahir, F., 2013. Effect of zeta potential on the properties of nano-drug delivery systems - a review (Part 2). Trop. J. Pharm. Res. 12, 265–273. doi:10.4314/tjpr.v12i2.20.

Hosseini, S.F., Zandi, M., Rezaei, M., Farahmandghavi, F., 2013. Two-step method for encapsulation of oregano essential oil in chitosan nanoparticles: preparation, characterization and *in vitro* release study. Carbohydr. Polym. 95, 50–56. doi:10.1016/J.CARBPOL.2013.02.031.

Hussein, J., El-Banna, M., Mahmoud, K.F., Morsy, S., Abdel Latif, Y., Medhat, D., Refaat, E., Farrag, A.R., El-Daly, S.M., 2017. The therapeutic effect of nano-encapsulated and nano-emulsion forms of carvacrol on experimental liver fibrosis. Biomed. Pharmacother. 90, 880–887. doi:10.1016/j.biopha.2017.04.020.

Iqbal, M., Valour, J.-P., Fessi, H., Elaissari, A., 2015. Preparation of biodegradable PCL particles via double emulsion evaporation method using ultrasound technique. Colloid Polym. Sci. 293, 861–873. doi:10.1007/s00396-014-3464-9.

Islam, M.T., da Mata, A.M.O.F., de Aguiar, R.P.S., Paz, M.F.C.J., de Alencar, M.V.O.B., Ferreira, P.M.P., de Carvalho Melo-Cavalcante, A.A., 2016. Therapeutic potential of essential oils focusing on diterpenes. Phyther. Res. 30, 1420–1444. doi:10.1002/ptr.5652.

Jenkins, P., Snowden, M., 1996. Depletion flocculation in colloidal dispersions. Adv. Colloid Interface Sci. 68, 57–96. doi:10.1016/S0001-8686(96)90046-9.

Jung, S.-M., Min, S.K., Lee, H.C., Kwon, Y.S., Jung, M.H., Shin, H.S., 2016. Spirulina -PCL nanofiber wound dressing to improve cutaneous wound healing by enhancing antioxidative mechanism. J. Nanomater. 2016, 1–10. doi:10.1155/2016/6135727.

Jütte, R., Heinrich, M., Helmstädter, A., Langhorst, J., Meng, G., Niebling, W., Pommerening, T., Trampisch, H.J., 2017. Herbal medicinal products – evidence and tradition from a historical perspective. J. Ethnopharmacol. 207, 220–225. doi:10.1016/J.JEP.2017.06.047.

Kalepu, S., Nekkanti, V., 2015. Insoluble drug delivery strategies: review of recent advances and business prospects. Acta Pharm. Sin. B 5, 442–453. doi:10.1016/J.APSB.2015.07.003.

Kaszuba, M., Corbett, J., Watson, F.M., Jones, A., 2010. High-concentration zeta potential measurements using light-scattering techniques. Philos. Trans. A. Math. Phys. Eng. Sci.Philos. Trans. A Math. Phys. Eng. Sci. 368, 4439–4451. doi:10.1098/rsta.2010.0175.

Khalifa, N.E., Nur, A.O., Osman, Z.A., 2017. Artemether loaded ethylcellulose nanosuspensions: effects of formulation variables, physical stability and drug release profile. Int. J. Pharm. Pharm. Sci. 9, 90. doi:10.22159/ijpps.2017v9i6.18321.

Khayata, N., Abdelwahed, W., Chehna, M.F., Charcosset, C., Fessi, H., 2012. ~~Preparation of vitamin E loaded nanocapsules by the nanoprecipitation method: From laboratory scale to large scale using a membrane contactor~~Preparation of vitamin E loaded nanocapsules by the nanoprecipitation method: from laboratory scale to large scale using a membrane contactor. Int. J. Pharm. 423, 419–427. doi:10.1016/j.ijpharm.2011.12.016.

~~Kostakova, E.K., Meszaros, L., Maskova, G., Blazkova, L., Turcsan, T., Lukas, D., 2017. Crystallinity of electrospun and centrifugal spun polycaprolactone fibers: a comparative study. doi:10.1155/2017/8952390.~~

Kostakova, E.K., Meszaros, L., Maskova, G., Blazkova, L., Turscan, T., Lukas, D., 2017. Cristallinity of electrospun and centrifugal spun polycaprolactone fibers: a comparative study. J. Nanomater. 2017, 1–9. doi:https://doi.org/10.1155/2017/8952390.

Labet, M., Thielemans, W., 2009. Synthesis of polycaprolactone: a review. Chem. Soc. Rev. 38, 3484. doi:10.1039/b820162p.

Liu, X., Diarra, M.S., Zhang, Y., Wang, Q., Yu, H., Nie, S.-P., Xie, M.-Y., Gong, J., 2016. Effect of encapsulated carvacrol on the incidence of necrotic enteritis in broiler chickens. Avian Pathol. 45, 357–364. doi:10.1080/03079457.2016.1138281.

~~Magenheim, B., Benita, S., 1991. Nanoparticle characterization: a comprehensive physicochemical approach.~~

Magenheim, B., Benita, S., 1991. Nanoparticle characterization: a comprehensive physicochemical approach.. STP Pharma. Sci. 1, 221–241.

Maia, J.L., Santana, M.H.A., Ré, M.I., 2004. The effect of some processing conditions on the characteristics of biodegradable microspheres obtained by an emulsion solvent evaporation process. ~~Brazilian J. Chem. Eng.~~Braz. J. Chem. Eng. 21, 01–12. doi:10.1590/S0104-66322004000100002.

Malikmammadov, E., Tanir, T.E., Kiziltay, A., Hasirci, V., Hasirci, N., 2018. PCL and PCL-based materials in biomedical applications. J. Biomater. Sci. Polym. Ed. 29, 863–893. doi:10.1080/09205063.2017.1394711.

Man, A., Santacroce, L., Jacob, R., Mare, A., Man, L., Man, A., Santacroce, L., Jacob, R., Mare, A., Man, L., 2019. Antimicrobial activity of six essential oils against a group of human pathogens: a comparative study. Pathogens 8, 15. doi:10.3390/pathogens8010015.

Martí, M., Martínez, V., Carreras, N., Alonso, C., Lis, M.J., Parra, J.L., Coderch, L., 2014. Textiles with gallic acid microspheres: *in vitro* release characteristics. J. Microencapsul. 31, 535–541. doi:10.3109/02652048.2014.885605.

Martínez Rivas, C.J., Tarhini, M., Badri, W., Miladi, K., Greige-Gerges, H., Nazari, Q.A., Galindo Rodríguez, S.A., Román, R., Fessi, H., Elaissari, A., 2017. Nanoprecipitation process: from

encapsulation to drug delivery. Int. J. Pharm. 532, 66–81. doi:10.1016/J.IJPHARM.2017.08.064.

Martucci, J.F., Gende, L.B., Neira, L.M., Ruseckaite, R.A., 2015. Oregano and lavender essential oils as antioxidant and antimicrobial additives of biogenic gelatin films. Ind. Crops Prod. 71, 205–213. doi:10.1016/J.INDCROP.2015.03.079.

Massaroni, C., Saccomandi, P., Schena, E., 2015. Medical smart textiles based on fiber optic technology: an overview. J. Funct. Biomater. 6, 204–221. doi:10.3390/jfb6020204.

Mečņika, V., Hoerr, M., Krieviņš, I., Drscing, A., Schwarz, A., 2014. Smart Textiles for Healthcare: Applications and Technologies. In: Rural Environment. Education. Personality., vol. 7. ~~Smart textiles for healthcare: applications and technologies~~Latvia University of Agriculture, pp. 150–161.

Miladi, K., Sfar, S., Fessi, H., Elaissari, A., 2016. Nanoprecipitation process: from particle preparation to *in vivo* applications. In: ~~in: olymer Nanoparticles for Nanomedicines~~Polymer Nanoparticles for Nanomedicines, Springer International Publishing, Cham, pp. 17–53. doi:10.1007/978-3-319-41421-8_2.

Mirbagheri, M., Mohebbi-kalhori, D., Jirofti, N., 2017. Evaluation of mechanical properties and medical applications of polycaprolactone small diameter artificial blood vessels. Int. J. Basic Sci. Med. 2, 58–70. doi:10.15171/ijbsm.2017.12.

Mora-Huertas, C.E., Fessi, H., Elaissari, A., 2010. Polymer-based nanocapsules for drug delivery. Int. J. Pharm. 385, 113–142. doi:10.1016/J.IJPHARM.2009.10.018.

Mossotti, R., Ferri, A., Innocenti, R., Zelenková, T., Dotti, F., Marchisio, D.L., Barresi, A.A., 2015. Cotton fabric functionalisation with menthol/PCL micro- and nano-capsules for comfort improvement. J. Microencapsul. 32, 650–660. doi:https://doi.org/10.3109/02652048.2015.1073386.

Nasr, M., Jalali Sendi, J., Moharramipour, S., Zibaee, A., 2017. Evaluation of *Origanum vulgare* L. essential oil as a source of toxicant and an inhibitor of physiological parameters in diamondback moth, *Plutella xylustella* L. (Lepidoptera: Pyralidae). J. Saudi Soc. Agric. Sci. 16, 184–190. doi:10.1016/J.JSSAS.2015.06.002.

Oliveira, S.P.L.F., Bertan, L.C., De Rensis, C.M.V.B., Bilck, A.P., Vianna, P.C.B., Oliveira, S.P.L.F., Bertan, L.C., De Rensis, C.M.V.B., Bilck, A.P., Vianna, P.C.B., 2017. Whey protein-based films incorporated with oregano essential oil. Polmeros 27, 158–164. doi:10.1590/0104-1428.02016.

Persenaire, O., Alexandre, M., Degée, P., Dubois , P., 2001. Mechanisms and kinetics of thermal degradation of poly(ε-caprolactone). Biomacromolecules 2, 288–294. doi: 10.1021/BM0056310.

~~Persenaire, O., Alexandre, M., Philippe Degée, A., Dubois †, P., 2001. Mechanisms and kinetics of thermal degradation of poly(ε-caprolactone), doi:10.1021/BM0056310.~~

Olmedo, R., Nepote, V., Grosso, N.R., 2014. Antioxidant activity of fractions from oregano essential oils obtained by molecular distillation. Food Chem. 156, 212–219.

doi:10.1016/j.foodchem.2014.01.087.

Orchard, A., van Vuuren, S., 2017. Commercial essential oils as potential antimicrobials to treat skin diseases. ~~Evidence-Based Complement. Altern. Med.~~ Evid. Complement. Alternat. Med. 2017, 1–92. doi:10.1155/2017/4517971.

Palla, B.J., Shah, D.O., 2002. Stabilization of high ionic strength slurries using surfactant mixtures: molecular factors that determine optimal stability. J. Colloid Interface Sci. 256, 143–152. doi:10.1006/jcis.2002.8648.

Piazzon Tagliari, M., Granada, A., Antonio Segatto Silva, M., Karine Stulzer, H., Giehl Zanetti-Ramos, B., Fernandes, D., Thais Silva, I., Maria Oliveira Simões, C., Sordi, R., Assreuy, J., Soldi, V., 2015. Development of oral nifedipine-loaded polymeric nanocapsules: physicochemical characterisation, photostability studies, *in vitro* and *in vivo* evaluation. Quim. Nov. 38, 781–786. doi:10.5935/0100-4042.20150076.

Pimentel-Moral, S., Verardo, V., Robert, P., Segura-Carretero, A., Martínez-Férez, A., 2016. Nanoencapsulation strategies applied to maximize target delivery of intact polyphenols. Encapsulations 559–595. doi:10.1016/B978-0-12-804307-3.00013-2.

Pohlmann, A.R., Fonseca, F.N., Paese, K., Detoni, C.B., Coradini, K., Beck, R.C., Guterres, S.S., 2013. Poly(ε-caprolactone) microcapsules and nanocapsules in drug delivery. Expert Opin. Drug Deliv. 10, 623–638. doi:10.1517/17425247.2013.769956.

~~de Sousa~~ Ribeiro, ~~V.~~ A.F., ~~de O. Ribeiro~~ de Oliveira Rezende, R.L., ~~Rezende~~ Cabral, L.M., ~~de Cabral~~ de Soussa, V.P., 2013. Poly ε-caprolactone nanoparticles loaded with *Uncaria tomentosa* extract: preparation, characterization, and optimization using the the Box–Behnken design. ~~Int. J. Nanomedicine~~ Int. J. Nanomed. 8, 431 ~~–442~~. doi:10.2147/IJN.S38491.

Rübe, A., Hause, G., Mäder, K., Kohlbrecher, J., 2005. Core-shell structure of miglyol/poly(d,l-lactide)/poloxamer nanocapsules studied by small-angle neutron scattering. J. Control. Release 107, 244–252. doi:10.1016/J.JCONREL.2005.06.005.

~~Ruela, A.L.M., Perissinato, A.G., Lino, M.L., Mudrik, P.S., Pereira, G.R., 2016. Evaluation of skin absorption of drugs from topical and transdermal formulations.~~

Ruela, A.L.M., Perissinato, A.G., Lino, M.L., Mudrik, P.S., Pereira, G.R., 2016. Evaluation of skin absorption of drugs from topical and transdermal formulations. Braz. J. Pharm. Sci. 52, 527–544. doi:https://doi.org/10.1590/s1984-82502016000300018.

Saeed, S., Tariq, P., 2009. Antibacterial activity of oregano (*Origanum vulgare Linn.*) against gram positive bacteria. Pak. J. Pharm. Sci. 22, 421–424.

Sarkic, A., Stappen, I., Sarkic, A., Stappen, I., 2018. Essential oils and their single compounds in cosmetics—a critical review. Cosmetics 5, 11. doi:10.3390/cosmetics5010011.

Seifriz, W., 1924. Studies in emulsions. III-V. J. Phys. Chem. 29, 738–749. doi:10.1021/j150252a009.

Shaaban, H.A.E., El-Ghorab, A.H., Shibamoto, T., 2012. The journal of essential oil research, Journal of essential oil research, Allured Publishing Corporation.

Shaaban, H.A.E., EL-Ghorab, A.H., Shibamoto, T., 2012. Bioactivity of essential oils and their volatile aroma components: Review. J. Essent. Oil Res. 24, 203–212. doi:https://doi.org/10.1080/10412905.2012.659528.

Sharifi-Rad, J., Sureda, A., Tenore, G., Daglia, M., Sharifi-Rad, M., Valussi, M., Tundis, R., Sharifi-Rad, M., Loizzo, M., Ademiluyi, A., Sharifi-Rad, R., Ayatollahi, S., Iriti, M., 2017. Biological activities of essential oils: from plant chemoecology to traditional healing systems. Molecules 22, 70. doi:10.3390/molecules22010070.

Silva, F.V., Guimarães, A.G., Silva, E.R.S., Sousa-Neto, B.P., Machado, F.D.F., Quintans-Júnior, L.J., Arcanjo, D.D.R., Oliveira, F.A., Oliveira, R.C.M., 2012. Anti-inflammatory and anti-ulcer activities of carvacrol, a monoterpene present in the essential oil of oregano. J. Med. Food 15, 984–991. doi:10.1089/jmf.2012.0102.

Singh, R., Lillard, J.W., Jr., 2009. Nanoparticle-based targeted drug delivery. Exp. Mol. Pathol. 86, 215–223. doi:10.1016/j.yexmp.2008.12.004.

Stander, B.A., van Vollenstee, F.A., Kallmeyer, K., Potgieter, M., Joubert, A., Swanepoel, A., Kotze, L., Moolman, S., Pepper, M.S., 2018. An *in vitro* and *in vivo* study on the properties of hollow polycaprolactone cell-delivery particles. PLoS One 13. doi:10.1371/journal.pone.0198248, e0198248.

Suntres, Z.E., Coccimiglio, J., Alipour, M., 2015. The bioactivity and toxicological actions of carvacrol. Crit. Rev. Food Sci. Nutr. 55, 304–318. doi:10.1080/10408398.2011.653458.

Swamy, M.K., Akhtar, M.S., Sinniah, U.R., 2016. Antimicrobial properties of plant essential oils against human pathogens and their mode of action: an updated review. Evid. Based. Complement. Alternat. Med.Evid. Complement. Alternat. Med. 2016, 1–21. doi:10.1155/2016/3012462, 3012462.

Teixeira, B., Marques, A., Ramos, C., Neng, N.R., Nogueira, J.M.F., Saraiva, J.A., Nunes, M.L., 2013. Chemical composition and antibacterial and antioxidant properties of commercial essential oils. Ind. Crops Prod. 43, 587–595. doi:10.1016/J.INDCROP.2012.07.069.

Teixeira, B., Marques, A., Ramos, C., Serrano, C., Matos, O., Neng, N.R., Nogueira, J.M.F., Saraiva, J.A., Nunes, M.L., 2013. Chemical composition and bioactivity of different oregano (*Origanum vulgare*) extracts and essential oil. J. Sci. Food Agric. 93, 2707–2714. doi:10.1002/jsfa.6089.

Valderrama, A.C.S., Rojas De, G.C., 2017. Traceability of active compounds of essential oils in antimicrobial food packaging using a chemometric method by ATR-FTIR. Am. J. Anal. Chem. 8, 726–741. doi:10.4236/ajac.2017.811053.

Vattem, D.A., Lin, Y.-T., Ghaedian, R., Shetty, K., 2005. Cranberry synergies for dietary management of *Helicobacter pylori* infections. Process Biochem. 40, 1583–1592. doi:10.1016/J.PROCBIO.2004.06.024.

Verma, D.D., Verma, S., Blume, G., Fahr, A., 2003. Particle size of liposomes influences dermal delivery of substances into skin. Int. J. Pharm. 258, 141–151.

Wang, P., Luo, Q., Qiao, H., Ding, H., Cao, Y., Yu, J., Liu, R., Zhang, Q., Zhu, H., Qu, L., 2017. ~~The Neuroprotective effects of carvacrol on ethanol-induced hippocampal neurons impairment via the antioxidative and antiapoptotic pathways~~The neuroprotective effects of carvacrol on ethanol-induced hippocampal neurons impairment via the antioxidative and antiapoptotic pathways. Oxid. Med. Cell. Longev. 2017, 1–17. doi:10.1155/2017/4079425.

~~Wegener, T., 2017. Patterns and trends in the use of herbal products, herbal medicine and herbal medicinal products. doi:10.15406/ijcam.2017.09.00317.~~

Wegener, T., 2017. Patterns and trends in the use of herbal products, herbal medicine and herbal medicinal products. Int. J. Complement. Altern. Med. 9. doi:https://doi.org/10.15406/ijcam.2017.09.00317.

Woodard, L.F., Jasman, R.L., 1985. Stable oil-in-water emulsions: preparation and use as vaccine vehicles for lipophilic adjuvants. Vaccine 3, 137–144. doi:10.1016/0264-410X(85)90063-5.

Zhao, R., Xu, J., Guo, B., 2017. Preparation and *in vitro* evaluation of biodegradable microspheres with narrow size distribution for pulmonary delivery. Indian J. Pharm. Sci. 79, 930–938. doi:https://doi.org/10.4172/pharmaceutical-sciences.1000310.

Zotti, M., Colaianna, M., Morgese, M.G., Tucci, P., Schiavone, S., Avato, P., Trabace, L., 2013. Carvacrol: from ancient flavoring to neuromodulatory agent. Molecules 18, 6161–6172. doi:10.3390/molecules18066161.

Graphical abstract
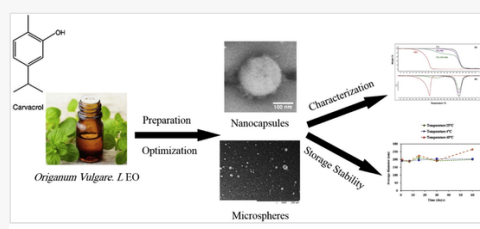
Highlights

- Encapsulation of oregano essential oil by nanoprecipitation and double emulsion.

- Nanocapsules showed a monomodal distribution and high encapsulation efficiency.

- Nanocapsules and microspheres physicochemical properties are maintained at 4 °C.

- Over 90% of retained carvacrol from nanocapsules at different temperatures.

- Microspheres' carvacrol retention decreased to 64.56% and 61.84% at 25 °C and 40 °C.

Queries and Answers

Query: Your article is registered as a regular item and is being processed for inclusion in a regular issue of the journal. If this is NOT correct and your article belongs to a Special Issue/Collection please contact a.noor@elsevier.com immediately prior to returning your corrections.
Answer: It's correct. The article belongs to a regular issue.

Query: The author names have been tagged as given names and surnames (surnames are highlighted in teal color). Please confirm if they have been identified correctly.
Answer: Yes

Query: Please confirm that the provided email is the correct address for official communication, else provide an alternate e-mail address to replace the existing one, because private e-mail addresses should not be used in articles as the address for communication.
Answer: It's the correct adress for official communication.

Query: Please check the presentation of affiliations and correct if necessary.
Answer: The presentation of affiliations is correct with some corrections done.

Query: Please note that Refs. "Zhao et al., 2017; Mossotti et al., 2015" are cited in the text but not provided in the reference list. Please provide them in the reference list or delete these citations from the text.
Answer: Refs Zhao et al., 2017 and Mossotti et al., 2015 are added and cited in the text.

Query: Please note that Table 6 was not cited in the text. Please check that the citation suggested is in the appropriate place and correct if necessary.

Answer: The suggested citation of table 6 was kept and an other citation of the same table was added.

Query: Have we correctly interpreted the following funding source(s) and country names you cited in your article: Tunisian Ministry of Higher Education and Scientific Research; Ministerio de Ciencia, Innovación y Universidades?

Answer: The funders order was changed. The Ministerio de Ciencia, Innovación y Universidades, Spain is the primary funder that has supported financially the experimental work.